Table 3. Treatment-Related Adverse Events (N = 37)

Adverse Event*	All Grades		Grade ≥ 3	
	No.	%	No.	%
Hematologic				
Lymphocytopenia	30	81	27	73
Leukocytopenia	16	43	5	14
Thrombocytopenia	14	38	1	3
Neutropenia	14	38	7	19
Anemia	5	14	2	5
Febrile neutropenia	1	3	1	3
Nonhematologic				
Pyrexia	11	30	0	0
Infusion reaction	9	24	0	0
ALT increased	8	22	1	3
ALP increased	8	22	1	3
Hypophosphatemia	6	16	1	3
Hypokalemia	2	5	1	3
Infection	1	3	1	3
Oral candidiasis	1	3	1	3
Pneumonia	1	3	1	3
Herpes esophagitis	1	3	1	3
Polymyositis	1	3	1	3
Second primary malignancy†	1	3	1	3
Skin and subcutaneous tissue disorders (SOC)	19	51	4	11
Rash papular	6	16	1	3
Rash erythematous	5	14	1	3
Psoriasis	2	5	1	3
Rash maculopapular	2	5	1	3
Toxic skin eruption	2	5	1	3

Abbreviations: ALP, alkaline phosphatase; SOC, System Organ Class (according to the Medical Dictionary for Regulatory Activities).
*Treatment-related adverse events that were reported in at least 15% of patients or that were of grade 3-4 severity.
†Diffuse large B-cell lymphoma was reported in one patient with angioimmunoblastic T-cell lymphoma.

mogamulizumab exhibited a profound depletion of the Treg cell subset during treatment, and cell levels had not returned to baseline 4 months after the last dose (Fig A1). Mogamulizumab also caused a modest decrease in the NK cell subset during treatment (data not shown).

DISCUSSION

This report described results from a single-arm, open-label multicenter phase II study of mogamulizumab in patients with relapsed CCR4-positive PTCL and CTCL.

Mogamulizumab showed promising antitumor activity, with an ORR of 35% (95% CI, 20% to 53%) and a CR/unconfirmed CR of 14%. These data were consistent with those reported with relapsed ATL.[30] It is notable that all three patients who relapsed after autoperipheral blood stem-cell transplantation responded to mogamulizumab. The total ORR is comparable to that of other US Food and Drug Administration-approved drugs, such as pralatrexate and romidepsin.[10,11] However, the present study differed from previous studies in several important respects. Firstly, the patient population was smaller than in the pralatrexate or romidepsin studies. Secondly, since it has been reported that CCR4 expression correlated with advanced disease,[24] it is important to note that although these two studies enrolled relapsed and refractory patients irrespective of their CCR4 expression status, the present study only recruited relapsed patients who were CCR4-positive. However, almost all patients in the present study had good PS compared with those patients in the previous studies. Thirdly, all patients with MF (n = 7) in the present study had relapsed after systemic chemotherapies and were presumed to have advanced stage disease, because all of these patients exhibited clinical skin tumors. Further, four of these seven patients exhibited clinically abnormal lymph node swelling, which does not usually occur at stages lower than IIB.[14,15]

In future study, PFS may also be improved by a longer continuous dosing schedule, such as a phase I/II study for CTCL.[31]

Although the number of patients was relatively small in the present study, the ORR for the AITL group (50%; six of 12) seemed noteworthy, while appearing relatively low in patients with PTCL-NOS (19%; three of 16). However, the three patients with PTCL-NOS who responded to mogamulizumab achieved durable PFS (9.0, 10.1+, and 10.8+ months; +, censored). Further studies are needed to identify which CCR4-positive T-cell lymphoma patients are most likely to benefit from mogamulizumab therapy.

There was no definite correlation between ORR and patient characteristics, such as age, CCR4 expression level, or number of previous systemic regimens. Although our study only included CCR4-positive patients with PTCL and CTCL, a recent US phase I/II study of mogamulizumab included both CCR4-positive and CCR4-negative patients with CTCL.[31] In that study, mogamulizumab exhibited efficacy irrespective of CCR4 expression (positive or negative) or CCR4 expression level, with a continuous dosing schedule.[31] Further studies are needed to define if CCR4 positivity represents a useful predictive biomarker in either PTCL or CTCL.

CCR4-positivity was confirmed in 78% of the 64 screened patients, a higher rate than previously reported.[20,21] However, it is possible that this variation in CCR4 positivity was due to differences in immunohistochemistry assay sensitivity. In our ongoing CTCL phase III study, our protocol permitted recruitment of both CCR4 positive and negative CTCL patients (NCT01728805). This is because the detection limit of CCR4 positivity may not be yet fully established, and mogamulizumab might have antitumor activity against CCR4-negative tumors through the depletion of CCR4-positive regulatory T cells,[36] thus enhancing pre-existing CD8+ cytolytic T-lymphocytes. Based on the latter new concept, an investigator-initiated trial of mogamulizumab against CCR4-negative solid tumors has been initiated (UMIN000010050).

Most of the AEs associated with mogamulizumab were mild and reversible. One patient suffered from polymyositis, an immune-related serious AE, after seven doses of mogamulizumab. The patient improved after steroid pulse therapy, treatment with tacrolimus hydrate, and continuous rehabilitation. Although drug-induced myositis was a possible cause, the relationship between mogamulizumab and myositis was not determined, even after detailed investigation. In our study, skin rash could also represent an immune-related AE, as other immunotherapies, including ipilimumab and zanolimumab, cause similar skin toxicity.[18,36-38] In addition, this may relate to the antitumor mechanism of mogamulizumab, because CCR4 contributes to skin-specific lymphocyte homing.[39] Indeed, a previous study revealed that patients who developed skin disorders ultimately had better therapeutic responses to treatment.[30] In the present study, of the

13 patients who developed grade 2 to 3 skin disorders, five patients achieved CR/PR. Of the 24 patients who developed grade 1 or no skin disorders, eight patients achieved CR/PR. Hence, no clear correlation between skin disorders and response rate was observed in the present study.

As shown in Figure A1, mogamulizumab caused a significant and persistent reduction in the number of Treg cells. This may be responsible for the increased incidence of skin disorders seen in patients with ATL.[30,40] Skin disorders were observed in 19 patients (51%), with grade 3/4 in four cases (11%). This was lower than the proportion of patients who developed skin disorders (67%, 22% in grade 3/4) in a previous study.[30] One patient (4%) with ATL developed Stevens-Johnson syndrome (SJS)[30] and four patients with ATL developed SJS/toxic epidermal necrolysis in postmarketing surveillance of mogamulizumab[40]; however, no cases of SJS/toxic epidermal necrolysis were observed in the present study. Similarly, four of 21 patients with ATL (19%) developed symptoms consistent with SJS[41] after treatment with pralatrexate, whereas no SJS was observed in patients with PTCL[10] after pralatrexate treatment. The risk of severe skin disorders may therefore be lower in patients with PTCL, compared with patients with ATL.

In conclusion, this phase II study revealed that mogamulizumab had promising efficacy and tolerability in patients with relapsed CCR4-positive PTCL and CTCL. Given its novel mechanism of action and favorable toxicity profile compared with multiagent cytotoxic chemotherapy, we might expect the use of mogamulizumab in combination with other agents. Further preclinical and clinical studies of combination therapy will be needed.

AUTHORS' DISCLOSURES OF POTENTIAL CONFLICTS OF INTEREST

Although all authors completed the disclosure declaration, the following author(s) and/or an author's immediate family member(s) indicated a financial or other interest that is relevant to the subject matter under consideration in this article. Certain relationships marked with a "U" are those for which no compensation was received; those relationships marked with a "C" were compensated. For a detailed description of the disclosure categories, or for more information about ASCO's conflict of interest policy, please refer to the Author Disclosure Declaration and the Disclosures of Potential Conflicts of Interest section in Information for Contributors.

Employment or Leadership Position: Shiro Akinaga, Kyowa Hakko Kirin (C) **Consultant or Advisory Role:** Michinori Ogura, Kyowa Hakko Kirin (C); Takashi Ishida, Kyowa Hakko Kirin (C); Kensei Tobinai, Kyowa Hakko Kirin (C); Kunihiro Tsukasaki, Kyowa Hakko Kirin (C); Junji Suzumiya, Kyowa Hakko Kirin (C); Hiroshi Inagaki, Kyowa Hakko Kirin (C); Kazuo Tamura, Kyowa Hakko Kirin (C); Masao Tomonaga, Kyowa Hakko Kirin (C) **Stock Ownership:** Shiro Akinaga, Kyowa Hakko Kirin **Honoraria:** Takashi Ishida, Kyowa Hakko Kirin; Ryuzo Ueda, Kyowa Hakko Kirin, Chugai Pharma **Research Funding:** Takashi Ishida, Kyowa Hakko Kirin; Kiyohiko Hatake, Kyowa Hakko Kirin; Masafumi Taniwaki, Kyowa Hakko Kirin; Kensei Tobinai, Kyowa Hakko Kirin; Mitsune Tanimoto, Kyowa Hakko Kirin; Kunihiro Tsukasaki, GlaxoSmithKline; Kenichi Ishizawa, Kyowa Hakko Kirin **Expert Testimony:** None **Patents, Royalties, and Licenses:** None **Other Remuneration:** Takashi Ishida, Kyowa Hakko Kirin; Ryuzo Ueda, Kyowa Hakko Kirin

AUTHOR CONTRIBUTIONS

Conception and design: Michinori Ogura, Takashi Ishida, Kiyohiko Hatake, Kensei Tobinai, Kunihiro Tsukasaki, Hiroshi Inagaki, Shiro Akinaga, Ryuzo Ueda
Financial support: Shiro Akinaga
Provision of study materials or patients: Michinori Ogura, Takashi Ishida, Kiyohiko Hatake, Masafumi Taniwaki, Kiyoshi Ando, Kensei Tobinai, Katsuya Fujimoto, Kazuhito Yamamoto, Toshihiro Miyamoto, Naokuni Uike, Mitsune Tanimoto, Kunihiro Tsukasaki, Kenichi Ishizawa
Collection and assembly of data: Michinori Ogura, Takashi Ishida, Kiyohiko Hatake, Masafumi Taniwaki, Kiyoshi Ando, Kensei Tobinai, Katsuya Fujimoto, Kazuhito Yamamoto, Toshihiro Miyamoto, Naokuni Uike, Mitsune Tanimoto, Kunihiro Tsukasaki, Kenichi Ishizawa
Data analysis and interpretation: Michinori Ogura, Takashi Ishida, Kensei Tobinai, Junji Suzumiya, Hiroshi Inagaki, Kazuo Tamura, Masao Tomonaga, Ryuzo Ueda
Manuscript writing: All authors
Final approval of manuscript: All authors

REFERENCES

1. WHO: WHO classification of tumours of haematopoietic and lymphoid tissues (ed 4). Lyon, France, International Agency for Research on Cancer (IARC), 2008
2. O'Leary HM, Savage KJ: Update on the World Health Organization classification of peripheral T-cell lymphomas. Curr Hematol Malig Rep 4:227-235, 2009
3. Vose J, Armitage J, Weisenburger D, et al: International peripheral T-cell and natural killer/T-cell lymphoma study: Pathology findings and clinical outcomes. J Clin Oncol 26:4124-4130, 2008
4. Lymphoma Study Group of Japanese Pathologists: The World Health Organization classification of malignant lymphomas in Japan: Incidence of recently recognized entities. Pathol Int 50:696-702, 2000
5. Aoki R, Karube K, Sugita Y, et al: Distribution of malignant lymphoma in Japan: Analysis of 2260 cases, 2001-2006. Pathol Int 58:174-182, 2008
6. Wollina U: Cutaneous T cell lymphoma: Update on treatment. Int J Dermatol 51:1019-1036, 2012
7. NCCN Clinical Practice Guidelines in Oncology. Non-Hodgkin's lymphomas. Version 1.2013. Fort Washington, PA, NCCN Clinical Practice Guidelines in Oncology, 2013
8. Savage KJ, Chhanabhai M, Gascoyne RD, et al: Characterization of peripheral T-cell lymphomas in a single North American institution by the WHO classification. Ann Oncol 15:1467-1475, 2004
9. Savage KJ: Therapies for peripheral T-cell lymphomas. Hematology Am Soc Hematol Educ Program 2011:515-524, 2011
10. O'Connor OA, Pro B, Pinter-Brown L, et al: Pralatrexate in patients with relapsed or refractory peripheral T-cell lymphoma: Results from the pivotal PROPEL study. J Clin Oncol 29:1182-1189, 2011
11. Coiffier B, Pro B, Prince HM, et al: Results from a pivotal, open-label, phase II study of romidepsin in relapsed or refractory peripheral T-cell lymphoma after prior systemic therapy. J Clin Oncol 30:631-636, 2012
12. Pro B, Advani R, Brice P, et al: Brentuximab vedotin (SGN-35) in patients with relapsed or refractory systemic anaplastic large-cell lymphoma: Results of a phase II study. J Clin Oncol 30:2190-2196, 2012
13. Sugaya M, Hamada T, Kawai K, et al: Guidelines for the management of cutaneous lymphomas (2011): A consensus statement by the Japanese Skin Cancer Society-Lymphoma Study Group. J Dermatol 40:2-14, 2013
14. Olsen E, Vonderheid E, Pimpinelli N, et al: Revisions to the staging and classification of mycosis fungoides and Sézary syndrome: A proposal of the International Society for Cutaneous Lymphomas (ISCL) and the cutaneous lymphoma task force of the European Organization of Research and Treatment of Cancer (EORTC). Blood 110:1713-1722, 2007
15. Kim YH, Liu HL, Mraz-Gernhard S, et al: Long-term outcome of 525 patients with mycosis fungoides and Sézary syndrome. Clinical prognostic factors and risk for disease progression. Arch Dermatol 139:857-866, 2003
16. Diamandidou E, Colome-Grimmer M, Fayad L, et al: Transformation of mycosis fungoides/Sezary syndrome: Clinical characteristics and prognosis. Blood 92:1150-1159, 1998
17. Olsen EA, Kim YH, Kuzel TM, et al: Phase IIB multicenter trial of vorinostat in patients with persistent, progressive, or treatment refractory cutaneous T-cell lymphoma. J Clin Oncol 25:3109-3115, 2007

18. Olsen E, Duvic M, Frankel A, et al: Pivotal phase III trial of two dose levels of denileukin diftitox for the treatment of cutaneous T-cell lymphoma. J Clin Oncol 19:376-388, 2001

19. Whittaker SJ, Demierre MF, Kim EJ, et al: Final results from a multicenter, international, pivotal study of romidepsin in refractory cutaneous T-cell lymphoma. J Clin Oncol 28:4485-4491, 2010

20. Jones D, O'Hara C, Kraus MD, et al: Expression pattern of T-cell-associated chemokine receptors and their chemokines correlates with specific subtypes of T-cell non-Hodgkin lymphoma. Blood 96:685-690, 2000

21. Ishida T, Inagaki H, Utsunomiya A, et al: CXC chemokine receptor 3 and CC chemokine receptor 4 expression in T-cell and NK-cell lymphomas with special reference to clinicopathological significance for peripheral T-cell lymphoma, unspecified. Clin Cancer Res 10:5494-5500, 2004

22. Ohshima K, Karube K, Kawano R, et al: Classification of distinct subtypes of peripheral T-cell lymphoma unspecified, identified by chemokine and chemokine receptor expression: Analysis of prognosis. Int J Oncol 25:605-613, 2004

23. Nakagawa M, Nakagawa-Oshiro A, Karnan S, et al: Array comparative genomic hybridization analysis of PTCL-U reveals a distinct subgroup with genetic alterations similar to lymphoma-type adult T-cell leukemia/lymphoma. Clin Cancer Res 15:30-38, 2009

24. Yagi H, Seo N, Ohshima A, et al: Chemokine receptor expression in cutaneous T cell and NK/T-cell lymphomas: Immunohistochemical staining and in vitro chemotactic assay. Am J Surg Pathol 30: 1111-1119, 2006

25. Shinkawa T, Nakamura K, Yamane N, et al: The absence of fucose but not the presence of galactose or bisecting N-acetylglucosamine of human IgG1 complex-type oligosaccharides shows the critical role of enhancing antibody-dependent cellular cytotoxicity. J Biol Chem 278:3466-3473, 2003

26. Niwa R, Sakurada M, Kobayashi Y, et al: Enhanced natural killer cell binding and activation by low-fucose IgG1 antibody results in potent antibody-dependent cellular cytotoxicity induction at lower antigen density. Clin Cancer Res 11:2327-2336, 2005

27. Niwa R, Shoji-Hosaka E, Sakurada M, et al: Defucosylated chimeric anti-CC chemokine receptor 4 IgG1 with enhanced antibody-dependent cellular cytotoxicity shows potent therapeutic activity to T-cell leukemia and lymphoma. Cancer Res 64:2127-2133, 2004

28. Yano H, Ishida T, Inagaki A, et al: Defucosylated anti CC chemokine receptor 4 monoclonal antibody combined with immunomodulatory cytokines: A novel immunotherapy for aggressive/refractory Mycosis fungoides and Sezary syndrome. Clin Cancer Res 13:6494-6500, 2007

29. Yamamoto K, Utsunomiya A, Tobinai K, et al: Phase I study of KW-0761, a defucosylated humanized anti-CCR4 antibody, in relapsed patients with adult T-cell leukemia-lymphoma and peripheral T-cell lymphoma. J Clin Oncol 28:1591-1598, 2010

30. Ishida T, Joh T, Uike N, et al: Defucosylated anti-CCR4 monoclonal antibody (KW-0761) for relapsed adult T-cell leukemia-lymphoma: A multicenter phase II study. J Clin Oncol 10:837-842, 2012

31. Duvic M, Pinter-Brown L, Foss F, et al: Results of a phase 1/2 study for KW-0761, a monoclonal antibody directed against CC chemokine receptor type 4 (CCR4), in CTCL patients. Presented at the 53rd Annual Meeting of the American Society of Hematology, San Diego, CA, December 10-13, 2011 (abstr 962)

32. Cheson BD, Horning SJ, Coiffier B, et al: Report of an international workshop to standardize response criteria for non-Hodgkin's lymphomas. J Clin Oncol 17:1244-1253, 1999

33. Tsukasaki K, Hermine O, Bazarbachi A, et al: Definition, prognostic factors, treatment, and response criteria of adult T-cell leukemia-lymphoma: A proposal from an international consensus meeting. J Clin Oncol 27:453-459, 2009

34. Stevens SR, Ke MS, Parry EJ, et al: Quantifying skin disease burden in mycosis fungoides-type cutaneous T-cell lymphomas: The severity-weighted assessment tool (SWAT). Arch Dermatol 138:42-48, 2002

35. Olsen EA, Whittaker S, Kim YH, et al: Clinical end points and response criteria in mycosis fungoides and Sézary syndrome: A consensus statement of the International Society for Cutaneous Lymphomas, the United States Cutaneous Lymphoma Consortium, and the Cutaneous Lymphoma Task Force of the European Organisation for Research and Treatment of Cancer. J Clin Oncol 29:2598-2607, 2011

36. Ishida T, Ueda R: CCR4 as a novel molecular target for immunotherapy of cancer. Cancer Sci 97:1139-1146, 2006

37. d'Amore F, Radford J, Relander T, et al: Phase II trial of zanolimumab (HuMax-CD4) in relapsed or refractory non-cutaneous peripheral T cell lymphoma. Br J Haematol 150:565-573, 2010

38. Hodi FS, O'Day JS, McDermott FD, et al: Improved survival with ipilimumab in patients with metastatic melanoma. N Engl J Med 363:711-723, 2010

39. Campbell JJ, Haraldsen G, Pan J, et al: The chemokine receptor CCR4 in vascular recognition by cutaneous but not intestinal memory T cells. Nature 400:776-780, 1999

40. Ishida T, Ito A, Sato F, et al: Stevens-Johnson syndrome associated with mogamulizumab treatment of adult T-cell leukemia/lymphoma. Cancer Sci 104:647-650, 2013

41. Lunning MA, Gonsky J, Ruan J, et al: Pralatrexate in relapsed/refractory HTLV-1 associated adult T-cell lymphoma/leukemia: A New York City multi-institutional experience. Blood 120 (ASH Annual Meeting). 2012 (abstr 2735)

Support

Sponsored by Kyowa Hakko Kirin (Tokyo, Japan).

Acknowledgment

Presented in part at the 54th Annual Meeting of the American Society of Hematology, Atlanta, GA, December 8-11, 2012. We thank Mayuko Okada-Kobayashi, MPharm, and Kouta Ohno, MPH (Kyowa Hakko Kirin) for their help in preparing this manuscript. This manuscript was proofread by Forte and International Documentation Center. We thank all the patients, their families, investigators, review committee members, medical experts, nurses, and clinical research coordinators who participated in this multicenter clinical trial.

Appendix

The following review committees and medical experts participated in this trial. Takashi Terauchi, Research Center for Cancer Prevention and Screening National Cancer Center; Ukihide Tateishi, Yokohama City University Graduate School of Medicine; Junichi Tsukada, University of Occupational and Environmental Health; Koichi Nakata, University of Occupational and Environmental Health; Shigeo Nakamura, Nagoya University Graduate School of Medicine; Koichi Ohshima, Kurume University School of Medicine; Tetsuo Nagatani, Hachioji Medical Center of Tokyo Medical University; Akimichi Morita, Nagoya City University Graduate School of Medical Sciences; Kuniaki Ito, National Cancer Center Hospital East; Noriko Usui, Jikei University School of Medicine; Hirokazu Nagai, Clinical Research Center National Hospital Organization Nagoya Medical Center.

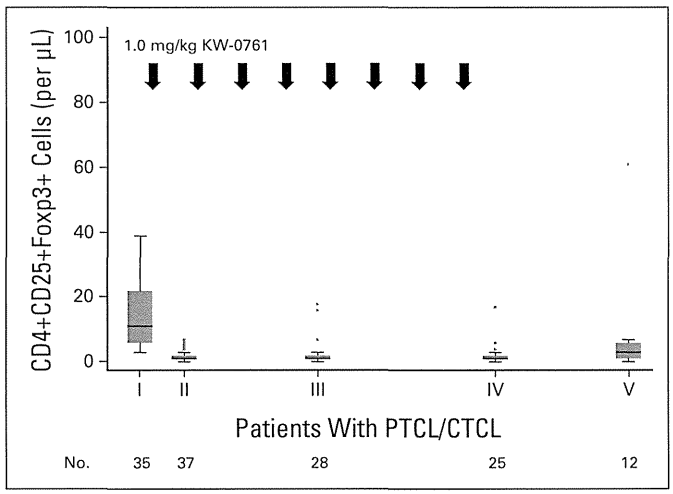

Fig A1. T-cell subset analysis. Numbers of CD4+CD25+Foxp3+ (regulatory T) cells are presented. Blood samples collected at times indicated in the protocol were analyzed. Blood samples were taken (I) just before the first mogamulizumab infusion, (II) just before the second infusion, (III) just before the fifth infusion, (IV) 1 week after the eighth infusion, and (V) 4 months after the eighth infusion. The number of samples used for analysis at each point is indicated below the graph. CTCL, cutaneous T-cell lymphoma; PTCL, peripheral T-cell lymphoma.

The Journal of Immunology

HTLV-1 bZIP Factor–Specific CD4 T Cell Responses in Adult T Cell Leukemia/Lymphoma Patients after Allogeneic Hematopoietic Stem Cell Transplantation

Tomoko Narita, Takashi Ishida, Ayako Masaki, Susumu Suzuki, Asahi Ito, Fumiko Mori, Tomiko Yamada, Masaki Ri, Shigeru Kusumoto, Hirokazu Komatsu, Yasuhiko Miyazaki, Yoshifusa Takatsuka, Atae Utsunomiya, Akio Niimi, Shinsuke Iida and Ryuzo Ueda

J Immunol 2014; 192:940-947; Prepublished online 20 December 2013;
doi: 10.4049/jimmunol.1301952
http://www.jimmunol.org/content/192/3/940

The Journal of Immunology is published twice each month by
The American Association of Immunologists, Inc.,
9650 Rockville Pike, Bethesda, MD 20814-3994.

Print ISSN: 0022-1767 Online ISSN: 1550-6606.

HTLV-1 bZIP Factor–Specific CD4 T Cell Responses in Adult T Cell Leukemia/Lymphoma Patients after Allogeneic Hematopoietic Stem Cell Transplantation

Tomoko Narita,* Takashi Ishida,* Ayako Masaki,* Susumu Suzuki,*,† Asahi Ito,* Fumiko Mori,* Tomiko Yamada,* Masaki Ri,* Shigeru Kusumoto,* Hirokazu Komatsu,* Yasuhiko Miyazaki,‡ Yoshifusa Takatsuka,§ Atae Utsunomiya,§ Akio Niimi,* Shinsuke Iida,* and Ryuzo Ueda†

We document human T lymphotropic virus type 1 (HTLV-1) bZIP factor (HBZ)-specific CD4 T cell responses in an adult T cell leukemia/lymphoma (ATL) patient after allogeneic hematopoietic stem cell transplantation (HCT) and identified a novel HLA-DRB1*15:01–restricted HBZ-derived naturally presented minimum epitope sequence, RRRAEKKAADVA (HBZ114–125). This peptide was also presented on HLA-DRB1*15:02, recognized by CD4 T cells. Notably, HBZ-specific CD4 T cell responses were only observed in ATL patients after allogeneic HCT (4 of 9 patients) and not in nontransplanted ATL patients (0 of 10 patients) or in asymptomatic HTLV-1 carriers (0 of 10 carriers). In addition, in one acute-type patient, HBZ-specific CD4 T cell responses were absent in complete remission before HCT, but they became detectable after allogeneic HCT. We surmise that HTLV-1 transmission from mothers to infants through breast milk in early life induces tolerance to HBZ and results in insufficient HBZ-specific T cell responses in HTLV-1 asymptomatic carriers or ATL patients. In contrast, after allogeneic HCT, the reconstituted immune system from donor-derived cells can recognize virus protein HBZ as foreign, and HBZ-specific immune responses are provoked that contribute to the graft-versus-HTLV-1 effect. *The Journal of Immunology*, **2014, 192: 940–947.**

Adult T cell leukemia/lymphoma (ATL) is a distinct hematologic malignancy caused by human T lymphotropic virus type 1 (HTLV-1) (1, 2). ATL is resistant to conventional chemotherapeutic agents, and only limited treatment options are available (3). Although early efforts using myeloablative chemoradiotherapy together with autologous hematopoietic stem cell rescue for ATL were associated with a high incidence of relapse and fatal toxicities (4), allogeneic hematopoietic stem cell transplantation (HCT) has been explored as a promising alternative treatment, achieving long-term remission in a proportion of patients with ATL (5, 6). The potential benefit of allogeneic HCT for ATL patients is considered to be due to the high immunogenicity of HTLV-1–infected cells (7–12), which was associated with the existence of posttransplant graft-versus-HTLV-1 and/or graft-versus-ATL effects (13, 14).

HTLV-1 was the first retrovirus to be directly associated with a human malignancy (15, 16), and ~20 million people worldwide are estimated to be infected with this virus (17). Among the HTLV-1 regulatory and accessory genes, *Tax* transforms rodent cells and immortalizes human primary T cells (18–20). In addition, Tax-transgenic mice develop spontaneous tumors (21–24). Another HTLV-1 component gene, *HBZ*, promotes the proliferation of ATL cells (25). Transgenic mice expressing HTLV-1 bZIP factor (HBZ) in their CD4 T cells share many symptoms and immunological features with HTLV-1–infected humans (26). Thus, both *Tax* and *HBZ* are thought to play critical roles in ATL oncogenesis, but there is a marked contrast between them in their expression profiles in primary ATL cells: HBZ expression is constitutive whereas Tax expression is frequently suppressed or minimal in ATL cells (25, 27, 28). Because immune responses against Tax were reported to be strong (7, 8), impaired Tax expression is thought to lead to a survival advantage for HTLV-1–infected cells in the host (2). These observations raise a simple question as to why the expression of Tax, but not HBZ, is impaired, despite both being HTLV-1–derived Ags seen by the human immune system as foreign. In other words, why is it that only HBZ, but not Tax, is constitutively expressed in ATL cells, although it was reported that HBZ is an immunogenic protein recognized by HBZ-specific CTL clones (29, 30). Although several studies (29–31) have been performed to determine the immunogenicity of HBZ, the precise immunological significance of HBZ in HTLV-1–infected individuals has not been fully established. Therefore, the aim of the current study was to clarify the clinical role of HBZ-specific immune responses in HTLV-1–infected individuals.

*Department of Medical Oncology and Immunology, Nagoya City University Graduate School of Medical Sciences, Nagoya 467-8601, Japan; †Department of Tumor Immunology, Aichi Medical University School of Medicine, Aichi 480-1195, Japan; ‡Department of Hematology, Oita Prefectural Hospital, Oita 870-8511, Japan; and §Department of Hematology, Imamura Bun-in Hospital, Kagoshima 890-0064, Japan

Received for publication July 22, 2013. Accepted for publication November 20, 2013.

This work was supported by grants-in-aid for scientific research (B) (No. 25290058) and scientific support programs for cancer research (No. 221S0001) from the Ministry of Education, Culture, Sports, Science and Technology of Japan, grants-in-aid from the National Cancer Center Research and Development Fund (No. 21-6-3), and H23- Third-Term Comprehensive Control Research for Cancer-general-011 from the Ministry of Health, Labour and Welfare, Japan (all to T.I.). Nagoya City University Graduate School of Medical Sciences received research grant support from Kyowa Hakko Kirin for research carried out by T.I.

Address correspondence and reprint requests to Dr. Takashi Ishida, Department of Medical Oncology and Immunology, Nagoya City University Graduate School of Medical Sciences, 1 Kawasumi, Mizuho-chou, Mizuho-ku, Nagoya, Aichi 467-8601, Japan. E-mail address: itakashi@med.nagoya-cu.ac.jp

Abbreviations used in this article: AC, asymptomatic carrier; ATL, adult T cell leukemia/lymphoma; CR, complete remission; HAM, human T lymphotropic virus type 1–associated myelopathy; HBZ, human T lymphotropic virus type 1 bZIP factor; HCT, hematopoietic stem cell transplantation; HTLV-1, human T lymphotropic virus type 1.

www.jimmunol.org/cgi/doi/10.4049/jimmunol.1301952

Materials and Methods

Primary human cells

Blood samples were obtained from healthy volunteers, HTLV-1 asymptomatic carriers (ACs), and ATL patients. Mononuclear cells were isolated with Ficoll-Paque (Pharmacia, Peapack, NJ). Genotyping of HLA-DR, HLA-DQ, and HLA-DP was performed using an WAKFlow HLA-typing kit (WAKUNAGA Pharmacy, Hiroshima, Japan). Diagnosis and classification of clinical subtypes of ATL were according to the criteria proposed by the Japan Lymphoma Study Group (32). All donors provided informed written consent before sampling, according to the Declaration of Helsinki, and the current study was approved by the institutional ethics committees of Nagoya City University Graduate School of Medical Sciences.

Cell lines

ATN-1, MT-1, TL-Om1, and ATL102 are ATL cell lines; MT-2, MT-4, and TL-Su are HTLV-1–immortalized lines; and K562 is a chronic myelogenous leukemia blast crisis cell line (8, 33). Genotyping of HLA-DR, HLA-DQ, and HAL-DP was performed using a WAKFlow HLA-typing kit.

Expansion of HBZ-specific T cells

PBMCs from ATL patients or HTLV-1 ACs were suspended in RPMI 1640 (Cell Science and Technology Institute, Sendai, Japan) supplemented with 10% human serum and 10 μM synthetic HBZ-derived peptides at a cell concentration of 2×10^6/ml. The peptides were purchased from Invitrogen (Carlsbad, CA). The cell suspension (2×10^6 cells) was cultured at 37°C in 5% CO_2 for 2 d, and an equal volume of RPMI 1640 supplemented with 100 IU/ml IL-2 was added. After subsequent culture for 5 d, an equal volume of ALyS505N (Cell Science and Technology Institute) supplemented with 100 IU/ml IL-2 was added, and the cells were cultured with appropriate medium (ALyS505N with 100 IU/ml IL-2) for an additional 7 d.

Abs and flow cytometry

PerCP-conjugated anti-CD8 mAb (SK1; eBioscience, San Diego, CA) and PE-conjugated anti-CD4 mAb [SFCI12T4D11 (T4); Beckman Coulter, Fullerton, CA] were used. For assessing HLA class II expression, PE-conjugated anti–HLA-DR (G46-6; BD Biosciences, San Jose, CA), anti–HLA-DQ (HLA-DQ1; BioLegend, San Diego, CA), or appropriate isotype-control mAbs were used. For intracellular IFN-γ and TNF-α staining, the expanded cells were cocultured with or without target cells or synthetic peptides at 37°C in 5% CO_2 for 3 h, after which brefeldin A (BD Biosciences) was added at 2 μg/ml. The cells were then incubated for an additional 2 h. Subsequently, they were fixed in 10% formaldehyde and stained with FITC-conjugated anti–IFN-γ (45.15; Beckman Coulter) or allophycocyanin-conjugated anti–TNF-α (MAb11; eBioscience) mAbs with 0.25% saponin for 60 min at room temperature. To determine HLA restriction, HLA-blocking experiments were conducted. The expanded cells were preincubated with 20 μg/ml anti–HLA-DR (L243; BioLegend), 20 μg/ml anti–HLA-DQ (1SPVL3; Beckman Coulter), or appropriate isotype control mAbs (20 μg/ml) at 37°C in 5% CO_2 for 1 h, after which they were stimulated with the peptide or the cell lines (ATN-1 and K562). Cells were analyzed on a FACSCalibur (BD Biosciences) with the aid of FlowJo software (Tree Star, Ashland, OR).

Quantitative RT-PCR

Total RNA was isolated with RNeasy Mini Kits (QIAGEN, Tokyo, Japan). Reverse transcription from the RNA to first-strand cDNA was carried out using High Capacity RNA-to-cDNA Kits (Applied Biosystems, Foster City, CA). *HBZ* and *β-actin* mRNA were amplified using TaqMan Gene Expression Assays with the aid of an Applied Biosystems StepOnePlus. The primer set for *HBZ* was as follows: sense, 5′-TCGACCTGAGCTTTAAACTTACCTAGA-3′ and antisense, 5′-GACACAGGCAAGCATCGAAA-3′. All values given are means of triplicate determinations.

Results

T cell responses against synthetic peptides overlapping by 10 aa and covering the entire sequence of the spliced HBZ protein

Because it was reported that HTLV-1 Tax-specific T cells were induced in some ATL patients after allogeneic HCT (10, 11), we initially tried to expand HBZ-specific T cells using PBMCs from an ATL patient who received allogeneic HCT with reduced-intensity conditioning and has been in complete remission (CR) for >3 y (patient #1 after HCT). PBMCs were stimulated with a mixture of 1 16-mer and 19 20-mer synthetic peptides overlapping by 10 aa and covering the entire sequence of the spliced HBZ protein (peptides number 1–20, Fig. 1), at a concentration of 10 μM each. The expanded cells were analyzed by forward scatter height and side scatter height levels, and the lymphocyte population was determined and plotted to show CD4 and CD8 positivity (Fig. 2A, *left panels*). The expanded CD8 T cells responded weakly to stimulation with these 20 overlapping peptides relative to controls without peptide stimulation, as assessed by IFN-γ production (Fig. 2A, *upper middle panels*) but not TNF-α (Fig. 2A, *lower middle panels*). In contrast, the expanded CD4 T cells responded to stimulation by the 20 overlapping peptides by producing both IFN-γ (Fig. 2A, *upper right panels*) and TNF-α (Fig. 2A, *lower right panels*). Because the response of the stimulated and expanded CD4 T cells was stronger than the CD8 response, we focused on the CD4 T cell response against HBZ in patient #1 after HCT.

PBMCs from this patient (#1 after HCT) were stimulated with a mixture of five overlapping peptides consisting of peptides 1–4, 5–8, 9–12, 13–16, and 17–20 (Fig. 1). The expanded CD4 T cells responded to the peptide mixture 9–12 better than to control (no peptides). They produced both IFN-γ (Fig. 2B, *upper panels*) and TNF-α (Fig. 2B, *lower panels*). The expanded CD4 T cells responded very weakly to the peptide mixtures 13–16 and 17–20 by producing TNF-α but not IFN-γ. No responses were observed against the peptide mixtures 1–4 or 5–8 (Fig. 2B). These data indicate that the epitope of HBZ recognized by CD4 T cells from the patient was present in peptides 9–12, within HBZ aa residues 81–130 (Fig. 1).

Next, PBMCs from the same patient were stimulated with four synthetic peptides: 9, 10, 11, and 12. The expanded CD4 T cells responded to peptide 12 by producing both IFN-γ (Fig. 2C, *upper panels*) and TNF-α (Fig. 2C, *lower panels*). The cells did not respond significantly to the other peptides (9, 10, or 11). These results narrow down the specific epitope of HBZ recognized by the CD4 T cells from the patient to a sequence within peptide 12: HBZ aa 111–130 (Fig. 1).

Determination of the minimum epitope sequence of HBZ recognized by CD4 T cells

Seven synthetic peptides (12-1, 12-2, 12-3, 12-4, 12-5, 12-6, 12-7) representing parts of peptide 12 were prepared (Fig. 3A). Responses of the CD4 T cells, which had been stimulated by peptide 12, to these different peptides were tested. The expanded CD4 T cells responded better to peptides 12, 12-1, 12-2, 12-3, and 12-4

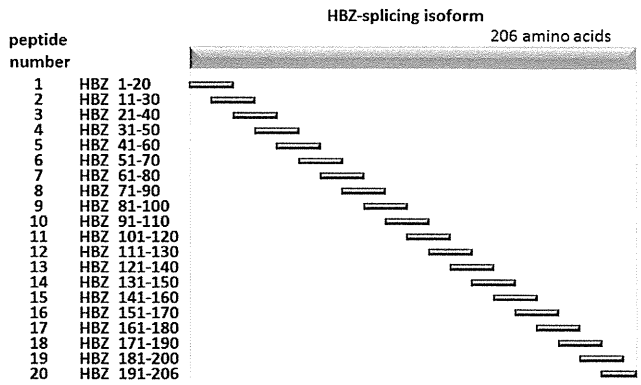

FIGURE 1. Synthetic peptides derived from spliced HBZ. Schematic of 19 20-mer and 1 16-mer synthetic peptides overlapping by 10 aa and covering the entire sequence of the spliced HBZ protein.

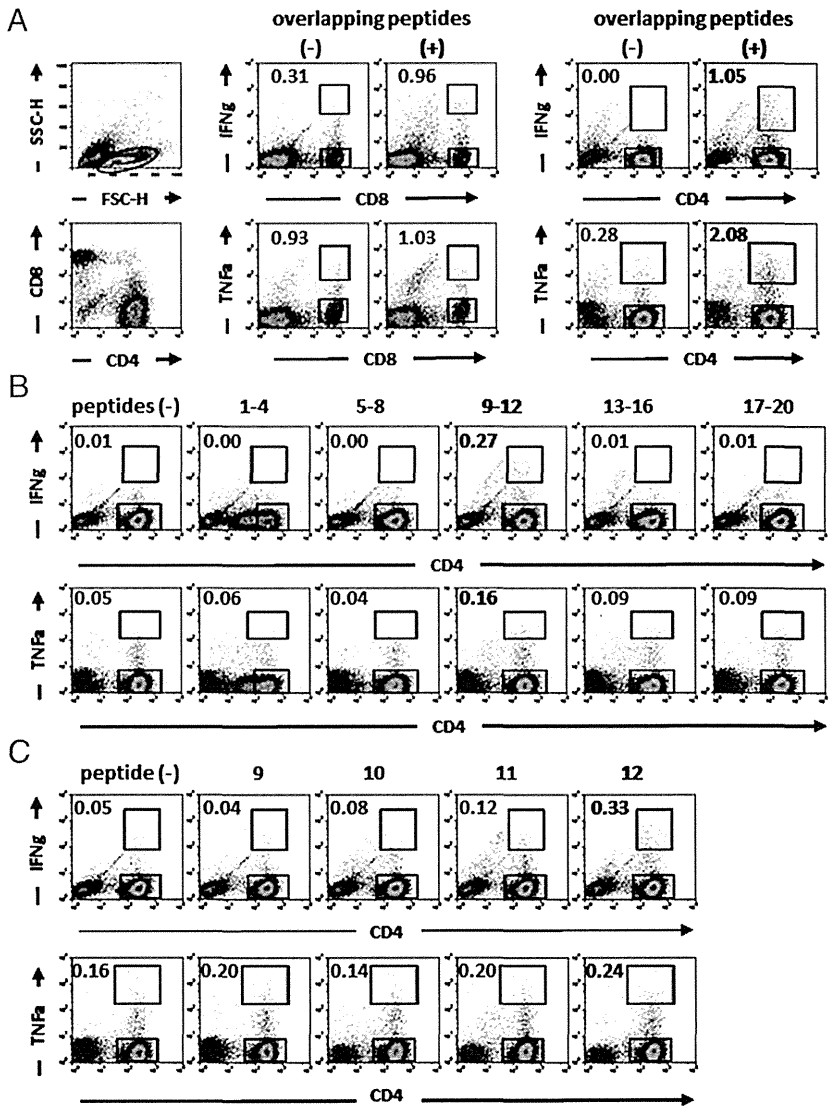

FIGURE 2. T cell responses against synthetic peptides overlapping by 10 aa and covering the entire sequence of the spliced HBZ protein. (**A**) PBMCs from patient #1 after HCT were expanded by stimulating with a mixture of 19 20-mer and 1 16-mer synthetic peptides overlapping by 10 aa and covering the entire sequence of the spliced HBZ protein. The responses of expanded CD8 and CD4 T cells to each of the overlapping peptides were evaluated by the production of IFN-γ or TNF-α. The percentage of responding cells in the upper gate ($CD8^+$ or $CD4^+$ and IFN-γ^+ or TNF-α^+ cells) relative to the cells in the lower gate ($CD8^+$ or $CD4^+$ and IFN-γ^- or TNF-α^- cells) is indicated in each flow cytometry panel. (**B**) PBMCs from patient #1 after HCT were expanded by stimulating with five overlapping peptide mixtures consisting of peptides 1–4, 5–8, 9–12, 13–16, and 17–20. (**C**) PBMCs from patient #1 after HCT were expanded by stimulating with four synthetic peptides: 9, 10, 11, and 12. The responses of expanded CD4 T cells to each synthetic peptide were evaluated by the production of IFN-γ or TNF-α. The percentage of responding cells in the upper gate relative to the cells in the lower gate is indicated in each flow cytometry panel. Each result is representative of three independent experiments.

by producing both IFN-γ and TNF-α. These cells did not respond to peptides 12-5, 12-6, or 12-7 (Fig. 3B). These data indicate that the N terminus of the minimum epitope sequence of HBZ recognized by the CD4 T cells from the patient is arginine, located at HBZ114 (Fig. 3A). Because the expanded CD4 T cells responded to peptide 12-4, the C terminus of the minimum epitope sequence of HBZ must be inside of alanine, located at HBZ125.

Next, three synthetic peptides (12-4-1, 12-4-2, 12-4-3; sequences were HBZ114–124, HBZ114–123, and HBZ114–122, respectively) were prepared to determine the C terminus of the minimum epitope sequence of HBZ (Fig. 3C). The expanded CD4 T cells responded to peptides 12-1 and 12-4 (positive controls) but not to 12-4-1, 12-4-2, 12-4-3, or a negative control peptide 12-7 (Fig. 3D). These data demonstrate that the minimum epitope sequence of HBZ recognized by the CD4 T cells from the patient was RRRAEKKAADVA (HBZ114–125).

Determination of the HLA allele on which the identified HBZ-derived peptides are presented to CD4 T cells

We investigated whether HBZ-specific CD4 T cells also recognized naturally processed and presented peptides. Thus, we initially determined *HBZ* expression by ATL or HTLV-1–immortalized cell lines and found that it was expressed by all of the lines tested (ATN-1, MT-1, MT-2, MT-4, TL-Su, TL-Om1, ATL102), regardless of their *Tax* mRNA expression (Fig. 4A, below the graph). *HBZ* expression levels of these established lines were almost as high as those of PBMCs containing >50% ATL cells obtained from 12 patients with the acute or chronic type of disease. K562 did not express *HBZ*, as might be expected, and all primary ATL cells tested were HBZ^+, consistent with an earlier study (Fig. 4A) (25). Next, we assessed the expression of HLA class II by the cell lines. The ATL or HTLV-1–immortalized cell lines tested were all positive for both HLA-DR and HLA-DQ (Fig. 4B). These observations indicate that ATN-1, MT-1, MT-2, MT-4, TL-Su, TL-Om1, and ATL102 had the potential to present the HBZ-derived peptides on their HLA-DR or HLA-DQ molecules.

Next, we examined the responses of HBZ-specific CD4 T cells from patient #1 after HCT against K562 or HBZ-expressing lines of different HLA types. The responses of HBZ-specific CD4 T cells to the lines were evaluated without the addition of peptide. The CD4 T cells that had been expanded from patient #1 after HCT using peptide 12 responded to peptide 12-1 (positive control) but not to K562, which expressed no *HBZ* (negative control) (Fig. 4C, *upper six panels*). When tested against ATL or HTLV-1–immortalized cell lines, the CD4 T cells responded strongly to ATN-1 and TL-Su (Fig. 4C, *lower panels*). Comparing the HLA class II types of the donor of the effector CD4 T cells (patient #1 after HCT) with ATN-1 and TL-Su showed that HLA-DRB1*15:01 and

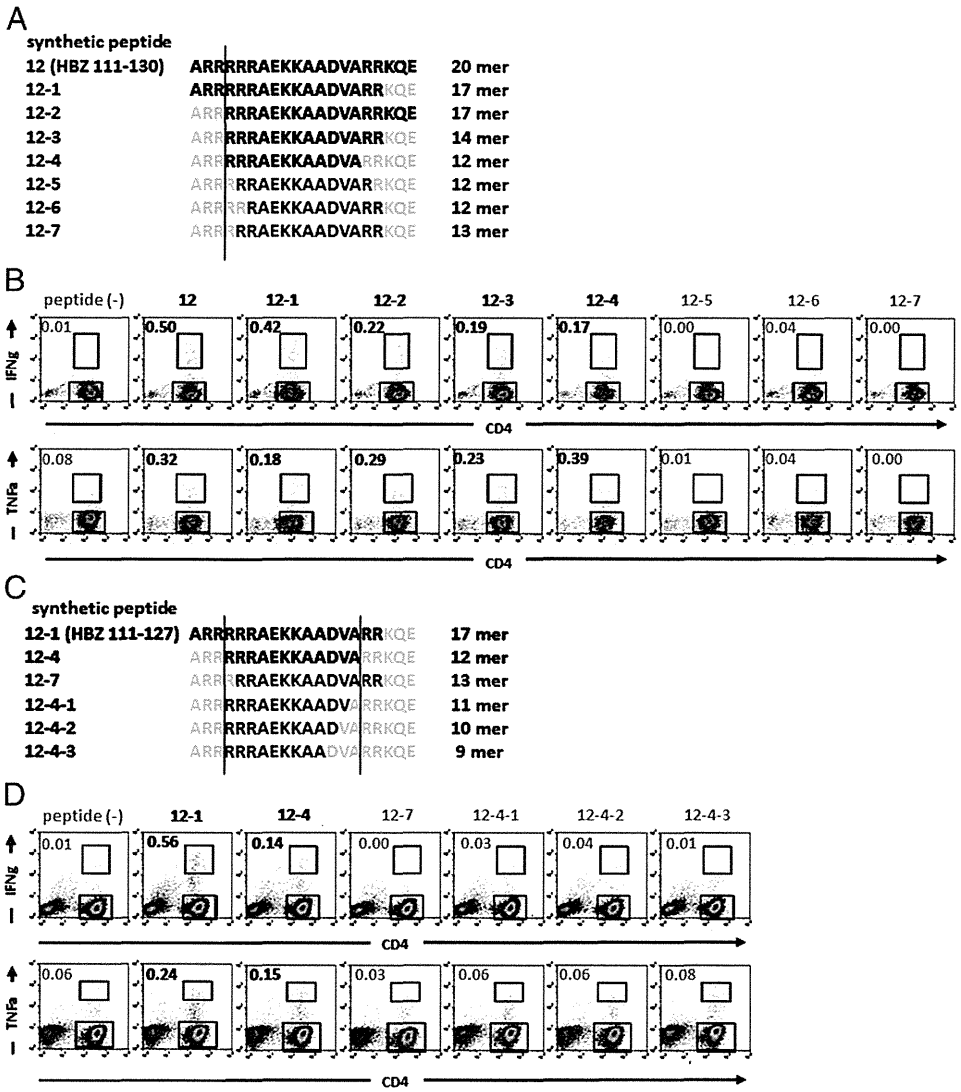

FIGURE 3. Determination of the minimum epitope sequence of HBZ recognized by CD4 T cells. (**A**) Schematic diagram of seven synthetic peptides (12-1, 12-2, 12-3, 12-4, 12-5, 12-6, 12-7) from peptide 12. They were prepared to determine the N terminus of the sequence representing the minimum epitope of HBZ recognized by the CD4 T cells. (**B**) PBMCs from patient #1 after HCT were expanded by peptide 12. The responses of expanded CD4 T cells to each synthetic peptide (12, 12-1, 12-2, 12-3, 12-4, 12-5, 12-6, 12-7) were evaluated by the production of IFN-γ or TNF-α. The percentage of responding cells in the upper gate relative to the cells in the lower gate is indicated in each flow cytometry panel. Each result is representative of three independent experiments. (**C**) Schematic diagram of three synthetic peptides (12-4-1, 12-4-2, 12-4-3) prepared to determine the C terminus of the sequence representing the minimum epitope of HBZ recognized by the CD4 T cells. (**D**) The responses of expanded CD4 T cells to each synthetic peptide (12-1, 12-4, 12-7, 12-4-1, 12-4-2, 12-4-3) were evaluated by the production of IFN-γ or TNF-α. The percentage of responding cells in the upper gate relative to the cells in the lower gate is indicated in each flow cytometry panel. Each result is representative of three independent experiments.

HLA-DQB1*06:02 were shared by all three (Table I). In addition, the CD4 T cells responded to MT-2, TL-Om1, and ATL102 to a lesser degree (Fig. 4C, *lower panels*); these three lines were found to share HLA-DRB1*15:02 and HLA-DQB1*06:01 (Table I). Together, these results indicate that the HBZ-specific CD4 T cell responses from patient #1 after HCT were restricted by HLA-DRB1*15:01 or HLA-DQB1*06:02, as well as by HLA-DRB1*15:02 or HLA-DQB1*06:01. In contrast, the peptide-sensitized CD4 T cells did not respond to MT-1 or MT-4 (Fig. 4C, *lower panels*), consistent with the present observations that the epitope of HBZ recognized by such CD4 T cells was restricted by HLA-DRB1*15:01/HLA-DQB1*06:02 and HLA-DRB1*15:02/HLA-DQB1*06:01.

Next, we tested whether HLA-DR or HLA-DQ restricted the presentation of the HBZ-derived peptide. CD4 T cells expanded by peptide 12 no longer responded to specific stimulation by peptide 12 in the presence of anti–HLA-DR–blocking mAb by producing IFN-γ (Fig. 5A, *upper left panels*), but it did respond in the presence of the isotype-control mAb (Fig. 5A, *upper right panels*). These CD4 T cells also still responded to peptide 12 in the presence of anti–HLA-DQ–blocking mAb (Fig. 5A, *lower left panels*) and its isotype control (Fig. 5A, *lower right panels*). In addition, in the presence of anti–HLA-DR–blocking mAb, CD4 T cells expanded by peptide 12 no longer responded to ATN-1 (Fig. 5B, *left panels*), which carried HLA-DRB1*15:01/HLA-DQB1*06:02 (Table I) and expressed *HBZ* mRNA (Fig. 4A). However, they did respond by producing IFN-γ and TNF-α in the presence of the isotype control (Fig. 5B, *left panels*). These CD4 T cells also still responded to ATN-1 in the presence of anti–HLA-DQ–blocking mAb and its isotype control (Fig. 5B, *right panels*). Furthermore, HBZ-specific CD4 T cell responses to K562 (negative control) were not affected by anti–HLA-DR, anti–HLA-DQ, or their isotype mAbs (Fig. 5C). These observations from Ab-blocking experiments, together with the results shown in Fig. 4, indicate that the epitope sequence of HBZ recognized by the CD4 T cells from patient #1 after HCT were restricted by HLA-DR, specifically HLA-DRB1*15:01 and HLA-DRB1*15:02.

Clinical significance of the specific CD4 T cell response against HBZ

The data presented thus far pertained to CD4 T cells obtained from only one patient (patient #1 after HCT). Therefore, we used HBZ peptide 12 to stimulate and expand 28 PBMC samples obtained from 27 other HTLV-1–infected individuals who carried HLA-DRB1*15:01 or HLA-DRB1*15:02. PBMCs were obtained from 10 HTLV-1 ACs, 10 ATL patients who had not undergone allogeneic HCT, and 8 ATL patients after allogeneic HCT. Among them, PBMCs from one individual (patient #2) were tested at different disease stages (i.e., CRs before and after allogeneic HCT). HBZ-specific CD4 T cell responses were absent in all 10

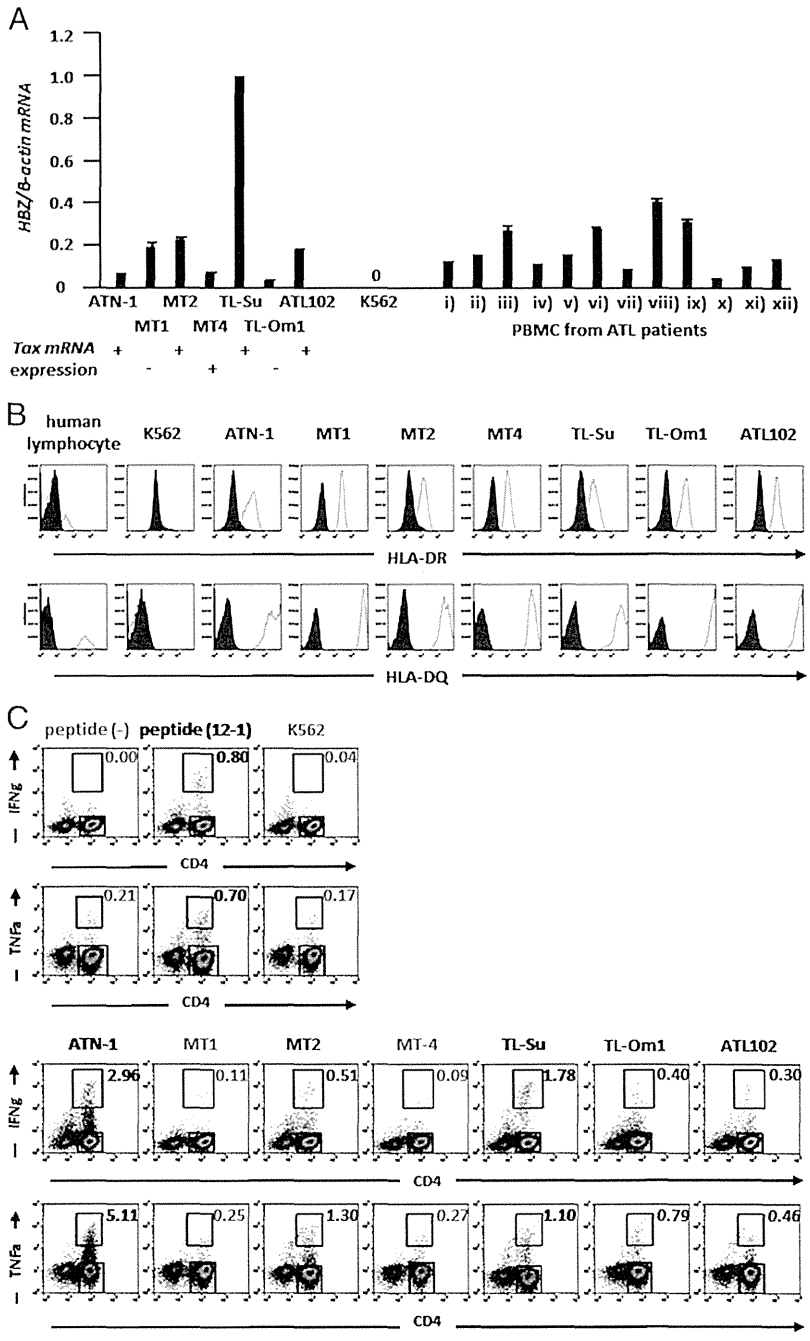

FIGURE 4. Responses of HBZ-specific CD4 T cells from patient #1 after HCT to ATL or HTLV-1–immortalized cell lines. (**A**) *HBZ* expression in ATL and HTLV-1–immortalized cell lines, K562, or PBMCs from ATL patients was analyzed by qRT-PCR by dividing the *HBZ* expression level by the *β-actin* expression level, resulting in an *HBZ/β-actin* mRNA ratio with the expression level in TL-Su set at unity. Data shown are means of triplicate experiments; error bars represent SD. *Tax* mRNA expression of each ATL and HTLV-1–immortalized cell line is indicated, as determined in our previous study (8). (**B**) HLA-DR and HLA-DQ expression in ATL cell lines, HTLV-1–immortalized lines, or K562, as analyzed by flow cytometry. The cell lines were stained with anti–HLA-DR mAb (*upper panels*, open graphs), anti–HLA-DQ mAb (*lower panels*, open graphs), or the corresponding isotype-control mAbs (filled graphs). (**C**) The expanded CD4 T cells were cocultured or not with the synthetic peptide 12-1. Negative controls without peptide stimulation (*upper left panels*) and positive controls with peptide stimulation (*upper middle panels*) are shown. The expanded CD4 T cells were cocultured with target cell lines in the absence of peptide stimulation. CD4 T cells did not respond to K562, which expressed no HBZ and acted as the negative control (*upper right panels*). The CD4 T cell responses to ATL or HTLV-1–immortalized cell lines, which expressed *HBZ*, with different HLA types were evaluated (*lower panels*). The percentage of responding cells in the upper gate relative to the cells in the lower gate is indicated in each flow cytometry panel. Each result is representative of three independent experiments.

HTLV-1 ACs, as well as in all 10 nontransplanted ATL patients (of whom 9 were in CR after systemic chemotherapy and the other was of smoldering type under observation only). In contrast, specific CD4 T cell responses to HBZ were observed in three of the eight additional ATL patients who were in CR after allogeneic HCT (patients #2, #3, and #4). The CD4 T cells from patient #2 and #4 after HCT responded to HBZ peptide 12 by producing both IFN-γ and TNF-α (Fig. 6, *right panels*). In patient #3, no TNF-α response was observed, but there was a clear IFN-γ response to HBZ peptide 12 (Fig. 6, *lower left panels*). Thus, specific CD4 T cell responses against HBZ were observed in four of nine recipients after allogeneic HCT (44%) but in no other ATL patients. Among the patients examined in this study, one patient with acute-type ATL received systemic chemotherapy and achieved CR. Subsequently, she received allogeneic HCT from an HLA-A, B, DR-matched HTLV-1 noninfected sibling donor and maintained CR (patient #2 after HCT). Although HBZ-specific CD4 T cell responses were not present at CR before allogeneic HCT in this patient (Fig. 6, *upper left panels*), they developed after transplantation (Fig. 6, *upper right panels*).

Table I. HLA information

	HLA-DRB1		HLA-DQB1		HLA-DPB1	
ATN-1	*04:05	*15:01	*04:01	*06:02	*05:01	*05:01
MT-1	*04:01	*09:01	*03:01	*03:03	*04:02	*05:01
MT-2	*04:04	*15:02	*03:02	*06:01	*05:01	*09:01
MT-4	*01:01	*16:02	*05:01	*05:02	*05:01	*05:01
TL-Su	*09:01	*15:01	*03:03	*06:02	*02:01	*17:01
TL-Om1	*15:02	*15:02	*06:01	*06:01	*09:01	*09:01
ATL102	*04:04	*15:02	*03:02	*06:01	*05:01	*09:01
Patient #1 after HCT	*04:05	*15:01	*04:01	*06:02	*02:01	*06:01

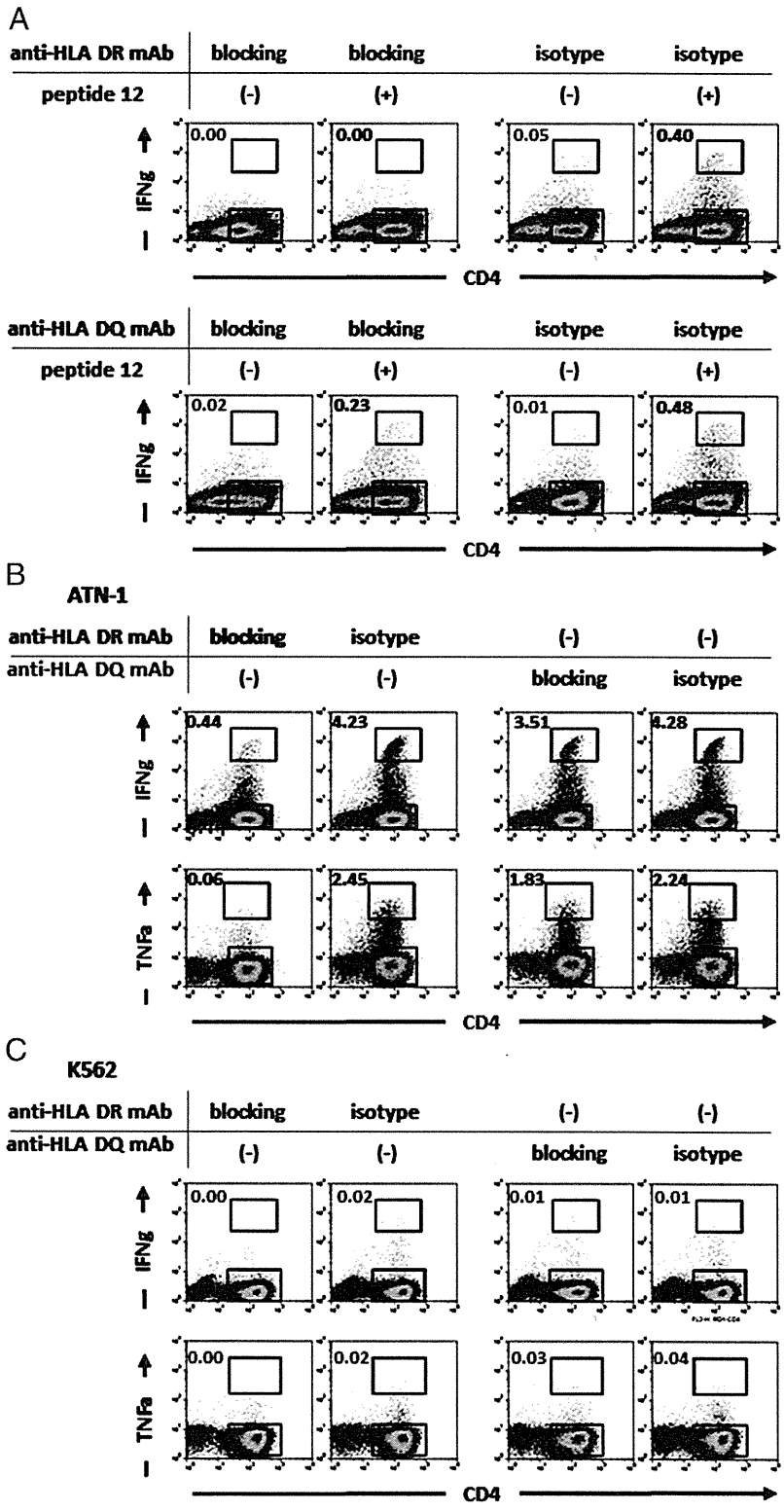

FIGURE 5. Determination of the HLA alleles restricting the presentation of HBZ-derived peptides to HBZ-specific CD4 T cells. (**A**) Responses of HBZ-specific CD4 T cells were evaluated, with or without HBZ peptide 12, in the presence of anti–HLA-DR–blocking mAb (*upper left panels*), anti–HLA-DQ–blocking mAb (*lower left panels*), or the corresponding isotype-control mAb (anti-HLA-DR isotype mAb, *upper right panels*; anti-HLA-DQ isotype mAb, *lower right panels*). Responses of HBZ-specific CD4 T cells to ATN-1, which carries HLA-DRB1*15:01/HLA-DQB1*06:02 and expresses *HBZ* mRNA (**B**), and to K562 (negative control) (**C**) were also evaluated in the presence of HLA-blocking mAbs or their isotype controls, without peptide stimulation. The percentage of responding cells in the upper gate relative to the cells in the lower gate is indicated in each flow cytometry panel. Each result is representative of three independent experiments.

Discussion

In the current study, we demonstrated the presence of HBZ-specific CD4 T cells in an ATL patient after allogeneic HCT and determined the minimum sequence of a novel HLA-DRB1*15:01–restricted HBZ-derived epitope to be RRRAEKKAADVA (HBZ114–125). HBZ peptides including the sequence HBZ114–125 were also presented on HLA-DRB1*15:02 and recognized by CD4 T cells. To the best of our knowledge, this is the first report to identify naturally processed and presented HLA-DR–restricted epitopes derived from HBZ on the surface of ATL cells. In an earlier study, an HBZ peptide–specific CTL line was established from an HLA-A*02:01^{+} individual, using peptides derived from the HBZ sequence. The peptides were selected by computer algorithms available at the BioInformatics and Molecular Analysis Section Web site (http://www-bimas.cit.nih.gov/molbio/hla_bind/) and the SYFPEITHI Web site (http://www.syfpeithi.de/) for strong binding affinity to the HLA-A*02:01 molecule. However, the established CTL line recognized the corresponding peptide-pulsed

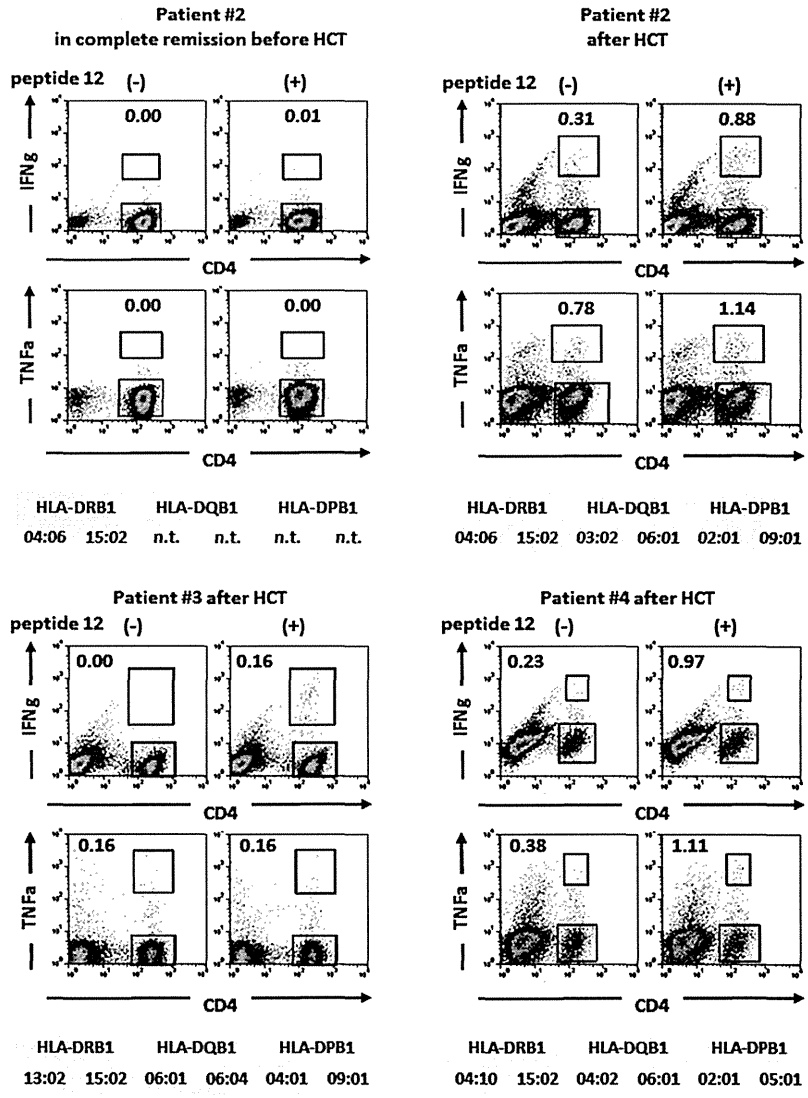

FIGURE 6. HBZ-specific CD4 T cell responses in additional ATL patients. PBMCs from additional ATL patients (#2, #3, and #4) carrying HLA-DRB1*15:02 were expanded by stimulation with HBZ peptide 12. The responses of expanded CD4 T cells to peptide 12 were evaluated by the production of IFN-γ or TNF-α. Although no HBZ-specific CD4 T cell response was observed in patient #2 in CR before allogeneic HCT (*upper left panels*), they developed after transplantation (*upper right panels*). HBZ-specific CD4 T cell responses were also observed in patient #3 (*lower left panels*) and patient #4 (*lower right panels*) in CR after allogeneic HCT. The percentage of responding cells in the upper gate relative to the cells in the lower gate is indicated in each flow cytometry panel. The HLA type of each patient is indicated below the flow cytometry panels. Each result is representative of three independent experiments. n.t., Not tested.

HLA-A*02:01$^+$ cells but not ATL cells (29). Therefore, it was not determined whether HBZ-derived peptides could be naturally presented on cells from HTLV-1–infected people. Another earlier study (30) demonstrated that HBZ expression was a critical determinant of viral persistence in the chronic phase of HTLV-1 infection. That novel study was performed using experimentally validated epitope-prediction software (34), but it did not determine the HBZ-derived epitope sequence or the corresponding HLA allele presenting it.

In the current study, no HLA-DRB1*15:01–restricted or HLA-DRB1*15:02–restricted HBZ-specific CD4 T cell response was observed in any ATL patients who had not undergone allogeneic HCT or in any HTLV-1 ACs. We surmise that HTLV-1 transmission from mothers to infants through breast milk in early life induces tolerance to HBZ, but not to Tax, by unknown mechanisms, resulting in insufficient HBZ-specific T cell responses in HTLV-1–infected individuals. This would be consistent with the persistent expression of HBZ in HTLV-1–infected cells (2, 25). In addition, insufficient HBZ-specific T cell responses may be due, in part, to the fact that the majority of the *HBZ* mRNA is retained in the nucleus, which may inhibit its translation (35), and probably leads to a low level of HBZ protein expression in HTLV-1–infected cells (29). In contrast, the finding that HLA-DRB1*15:01–restricted or HLA-DRB1*15:02–restricted HBZ-specific CD4 T cell responses were detected in ATL patients after allogeneic HCT requires explanation. Our hypothesis is that, after allogeneic HCT, the reconstituted immune system from donor-derived hematopoietic stem cells can recognize virus protein HBZ as foreign, although its expression is low, and HBZ-specific immune responses are provoked because of the lack of tolerance induction under these circumstances. In one patient with acute-type disease, HBZ-specific CD4 T cell responses were not observed in PBMCs at the time of CR before HCT, but they became detectable after allogeneic HCT. This observation supports our hypothesis. An earlier study (36) reported that HBZ-specific T cell responses were detected in some patients with HTLV-1–associated myelopathy (HAM). Unlike ATL, HAM can occur in individuals infected with HTLV-1 by any route of transmission, such as sexual intercourse (37). Therefore, some patients with HAM, infected with HTLV-1 after reaching adulthood (i.e., who became infected after their immune system had fully matured), may recognize virus protein HBZ as foreign, and HBZ-specific immune responses may be provoked. From this point of view, detection of HBZ-specific T cell responses might be expected in some HTLV-1 ACs, infected after becoming adults, but we did not see this in the present study.

In conclusion, we report the presence of HBZ-specific CD4 T cell responses in ATL patients who were in CR but only after allogeneic HCT. These responses potentially contribute to the

graft-versus-HTLV-1 effect. Novel strategies that enhance the posttransplantation allogeneic anti–HTLV-1 effect targeting HBZ, which never provokes graft-versus-host disease, could lead to improved outcomes of allogeneic HCT for ATL.

Acknowledgments

We thank Chiori Fukuyama for excellent technical assistance and Naomi Ochiai for excellent secretarial assistance.

Disclosures

T.I. received honoraria from Kyowa Hakko Kirin. The other authors have no financial conflicts of interest.

References

1. Uchiyama, T., J. Yodoi, K. Sagawa, K. Takatsuki, and H. Uchino. 1977. Adult T-cell leukemia: clinical and hematologic features of 16 cases. *Blood* 50: 481–492.
2. Matsuoka, M., and K. T. Jeang. 2007. Human T-cell leukaemia virus type 1 (HTLV-1) infectivity and cellular transformation. *Nat. Rev. Cancer* 7: 270–280.
3. Ishida, T., and R. Ueda. 2011. Antibody therapy for Adult T-cell leukemia-lymphoma. *Int. J. Hematol.* 94: 443–452.
4. Tsukasaki, K., T. Maeda, K. Arimura, J. Taguchi, T. Fukushima, Y. Miyazaki, Y. Moriuchi, K. Kuriyama, Y. Yamada, and M. Tomonaga. 1999. Poor outcome of autologous stem cell transplantation for adult T cell leukemia/lymphoma: a case report and review of the literature. *Bone Marrow Transplant.* 23: 87–89.
5. Utsunomiya, A., Y. Miyazaki, Y. Takatsuka, S. Hanada, K. Uozumi, S. Yashiki, M. Tara, F. Kawano, Y. Saburi, H. Kikuchi, et al. 2001. Improved outcome of adult T cell leukemia/lymphoma with allogeneic hematopoietic stem cell transplantation. *Bone Marrow Transplant.* 27: 15–20.
6. Ishida, T., M. Hishizawa, K. Kato, R. Tanosaki, T. Fukuda, S. Taniguchi, T. Eto, Y. Takatsuka, Y. Miyazaki, Y. Moriuchi, et al. 2012. Allogeneic hematopoietic stem cell transplantation for adult T-cell leukemia-lymphoma with special emphasis on preconditioning regimen: a nationwide retrospective study. *Blood* 120: 1734–1741.
7. Akimoto, M., T. Kozako, T. Sawada, K. Matsushita, A. Ozaki, H. Hamada, H. Kawada, M. Yoshimitsu, M. Tokunaga, K. Haraguchi, et al. 2007. Anti-HTLV-1 tax antibody and tax-specific cytotoxic T lymphocyte are associated with a reduction in HTLV-1 proviral load in asymptomatic carriers. *J. Med. Virol.* 79: 977–986.
8. Suzuki, S., A. Masaki, T. Ishida, A. Ito, F. Mori, F. Sato, T. Narita, M. Ri, S. Kusumoto, H. Komatsu, et al. 2012. Tax is a potential molecular target for immunotherapy of adult T-cell leukemia/lymphoma. *Cancer Sci.* 103: 1764–1773.
9. Masaki, A., T. Ishida, S. Suzuki, A. Ito, F. Mori, F. Sato, T. Narita, T. Yamada, M. Ri, S. Kusumoto, et al. 2013. Autologous Tax-specific CTL therapy in a primary adult T cell leukemia/lymphoma cell-bearing NOD/Shi-scid, IL-2Rγnull mouse model. *J. Immunol.* 191: 135–144.
10. Harashima, N., K. Kurihara, A. Utsunomiya, R. Tanosaki, S. Hanabuchi, M. Masuda, T. Ohashi, F. Fukui, A. Hasegawa, T. Masuda, et al. 2004. Graft-versus-Tax response in adult T-cell leukemia patients after hematopoietic stem cell transplantation. *Cancer Res.* 64: 391–399.
11. Tamai, Y., A. Hasegawa, A. Takamori, A. Sasada, R. Tanosaki, I. Choi, A. Utsunomiya, Y. Maeda, Y. Yamano, T. Eto, et al. 2013. Potential contribution of a novel Tax epitope-specific CD4+ T cells to graft-versus-Tax effect in adult T cell leukemia patients after allogeneic hematopoietic stem cell transplantation. *J. Immunol.* 190: 4382–4392.
12. Nishikawa, H., Y. Maeda, T. Ishida, S. Gnjatic, E. Sato, F. Mori, D. Sugiyama, A. Ito, Y. Fukumori, A. Utsunomiya, et al. 2012. Cancer/testis antigens are novel targets of immunotherapy for adult T-cell leukemia/lymphoma. *Blood* 119: 3097–3104.
13. Itonaga, H., H. Tsushima, J. Taguchi, T. Fukushima, H. Taniguchi, S. Sato, K. Ando, Y. Sawayama, E. Matsuo, R. Yamasaki, et al. 2013. Treatment of relapsed adult T-cell leukemia/lymphoma after allogeneic hematopoietic stem cell transplantation: the Nagasaki Transplant Group experience. *Blood* 121: 219–225.
14. Ishida, T., M. Hishizawa, K. Kato, R. Tanosaki, T. Fukuda, Y. Takatsuka, T. Eto, Y. Miyazaki, M. Hidaka, N. Uike, et al. 2013. Impact of Graft-versus-Host Disease on Allogeneic Hematopoietic Cell Transplantation for Adult T Cell Leukemia-Lymphoma Focusing on Preconditioning Regimens: Nationwide Retrospective Study. *Biol. Blood Marrow Transplant.* 19: 1731–1739.
15. Poiesz, B. J., F. W. Ruscetti, A. F. Gazdar, P. A. Bunn, J. D. Minna, and R. C. Gallo. 1980. Detection and isolation of type C retrovirus particles from fresh and cultured lymphocytes of a patient with cutaneous T-cell lymphoma. *Proc. Natl. Acad. Sci. USA* 77: 7415–7419.
16. Hinuma, Y., K. Nagata, M. Hanaoka, M. Nakai, T. Matsumoto, K. I. Kinoshita, S. Shirakawa, and I. Miyoshi. 1981. Adult T-cell leukemia: antigen in an ATL cell line and detection of antibodies to the antigen in human sera. *Proc. Natl. Acad. Sci. USA* 78: 6476–6480.
17. Gonçalves, D. U., F. A. Proietti, J. G. Ribas, M. G. Araújo, S. R. Pinheiro, A. C. Guedes, and A. B. Carneiro-Proietti. 2010. Epidemiology, treatment, and prevention of human T-cell leukemia virus type 1-associated diseases. *Clin. Microbiol. Rev.* 23: 577–589.
18. Grassmann, R., C. Dengler, I. Müller-Fleckenstein, B. Fleckenstein, K. McGuire, M. C. Dokhelar, J. G. Sodroski, and W. A. Haseltine. 1989. Transformation to continuous growth of primary human T lymphocytes by human T-cell leukemia virus type I X-region genes transduced by a Herpesvirus saimiri vector. *Proc. Natl. Acad. Sci. USA* 86: 3351–3355.
19. Tanaka, A., C. Takahashi, S. Yamaoka, T. Nosaka, M. Maki, and M. Hatanaka. 1990. Oncogenic transformation by the tax gene of human T-cell leukemia virus type I in vitro. *Proc. Natl. Acad. Sci. USA* 87: 1071–1075.
20. Akagi, T., and K. Shimotohno. 1993. Proliferative response of Tax1-transduced primary human T cells to anti-CD3 antibody stimulation by an interleukin-2-independent pathway. *J. Virol.* 67: 1211–1217.
21. Hinrichs, S. H., M. Nerenberg, R. K. Reynolds, G. Khoury, and G. Jay. 1987. A transgenic mouse model for human neurofibromatosis. *Science* 237: 1340–1343.
22. Nerenberg, M., S. H. Hinrichs, R. K. Reynolds, G. Khoury, and G. Jay. 1987. The tat gene of human T-lymphotropic virus type 1 induces mesenchymal tumors in transgenic mice. *Science* 237: 1324–1329.
23. Hasegawa, H., H. Sawa, M. J. Lewis, Y. Orba, N. Sheehy, Y. Yamamoto, T. Ichinohe, Y. Tsunetsugu-Yokota, H. Katano, H. Takahashi, et al. 2006. Thymus-derived leukemia-lymphoma in mice transgenic for the Tax gene of human T-lymphotropic virus type I. *Nat. Med.* 12: 466–472.
24. Ohsugi, T., T. Kumasaka, S. Okada, and T. Urano. 2007. The Tax protein of HTLV-1 promotes oncogenesis in not only immature T cells but also mature T cells. *Nat. Med.* 13: 527–528.
25. Satou, Y., J. Yasunaga, M. Yoshida, and M. Matsuoka. 2006. HTLV-I basic leucine zipper factor gene mRNA supports proliferation of adult T cell leukemia cells. *Proc. Natl. Acad. Sci. USA* 103: 720–725.
26. Satou, Y., J. Yasunaga, T. Zhao, M. Yoshida, P. Miyazato, K. Takai, K. Shimizu, K. Ohshima, P. L. Green, N. Ohkura, et al. 2011. HTLV-1 bZIP factor induces T-cell lymphoma and systemic inflammation in vivo. *PLoS Pathog.* 7: e1001274.
27. Fan, J., G. Ma, K. Nosaka, J. Tanabe, Y. Satou, A. Koito, S. Wain-Hobson, J. P. Vartanian, and M. Matsuoka. 2010. APOBEC3G generates nonsense mutations in human T-cell leukemia virus type 1 proviral genomes in vivo. *J. Virol.* 84: 7278–7287.
28. Takeda, S., M. Maeda, S. Morikawa, Y. Taniguchi, J. Yasunaga, K. Nosaka, Y. Tanaka, and M. Matsuoka. 2004. Genetic and epigenetic inactivation of tax gene in adult T-cell leukemia cells. *Int. J. Cancer* 109: 559–567.
29. Suemori, K., H. Fujiwara, T. Ochi, T. Ogawa, M. Matsuoka, T. Matsumoto, J. M. Mesnard, and M. Yasukawa. 2009. HBZ is an immunogenic protein, but not a target antigen for human T-cell leukemia virus type 1-specific cytotoxic T lymphocytes. *J. Gen. Virol.* 90: 1806–1811.
30. Macnamara, A., A. Rowan, S. Hilburn, U. Kadolsky, H. Fujiwara, K. Suemori, M. Yasukawa, G. Taylor, C. R. Bangham, and B. Asquith. 2010. HLA class I binding of HBZ determines outcome in HTLV-1 infection. *PLoS Pathog.* 6: e1001117.
31. Enose-Akahata, Y., A. Abrams, R. Massoud, I. Bialuk, K. R. Johnson, P. L. Green, E. M. Maloney, and S. Jacobson. 2013. Humoral immune response to HTLV-1 basic leucine zipper factor (HBZ) in HTLV-1-infected individuals. *Retrovirology* 10: 19.
32. Shimoyama, M. 1991. Diagnostic criteria and classification of clinical subtypes of adult T-cell leukaemia-lymphoma. A report from the Lymphoma Study Group (1984-87). *Br. J. Haematol.* 79: 428–437.
33. Ishida, T., A. Utsunomiya, S. Iida, H. Inagaki, Y. Takatsuka, S. Kusumoto, G. Takeuchi, S. Shimizu, M. Ito, H. Komatsu, et al. 2003. Clinical significance of CCR4 expression in adult T-cell leukemia/lymphoma: its close association with skin involvement and unfavorable outcome. *Clin. Cancer Res.* 9: 3625–3634.
34. MacNamara, A., U. Kadolsky, C. R. Bangham, and B. Asquith. 2009. T-cell epitope prediction: rescaling can mask biological variation between MHC molecules. *PLOS Comput. Biol.* 5: e1000327.
35. Rende, F., I. Cavallari, A. Corradin, M. Silic-Benussi, F. Toulza, G. M. Toffolo, Y. Tanaka, S. Jacobson, G. P. Taylor, D. M. D'Agostino, et al. 2011. Kinetics and intracellular compartmentalization of HTLV-1 gene expression: nuclear retention of HBZ mRNAs. *Blood* 117: 4855–4859.
36. Hilburn, S., A. Rowan, M. A. Demontis, A. MacNamara, B. Asquith, C. R. Bangham, and G. P. Taylor. 2011. In vivo expression of human T-lymphotropic virus type 1 basic leucine-zipper protein generates specific CD8+ and CD4+ T-lymphocyte responses that correlate with clinical outcome. *J. Infect. Dis.* 203: 529–536.
37. Yamano, Y., and T. Sato. 2012. Clinical pathophysiology of human T-lymphotropic virus-type 1-associated myelopathy/tropical spastic paraparesis. *Front. Microbiol.* 3: 389.

Published OnlineFirst April 11, 2014; DOI: 10.1158/1078-0432.CCR-13-3169

Human Cancer Biology

Clinical Cancer Research

CADM1 Expression and Stepwise Downregulation of CD7 Are Closely Associated with Clonal Expansion of HTLV-I–Infected Cells in Adult T-cell Leukemia/Lymphoma

Seiichiro Kobayashi[1], Kazumi Nakano[5], Eri Watanabe[2], Tomohiro Ishigaki[2], Nobuhiro Ohno[3], Koichiro Yuji[3], Naoki Oyaizu[4], Satomi Asanuma[5], Makoto Yamagishi[5], Tadanori Yamochi[5], Nobukazu Watanabe[2], Arinobu Tojo[1,3], Toshiki Watanabe[5], and Kaoru Uchimaru[3]

Abstract

Purpose: Cell adhesion molecule 1 (CADM1), initially identified as a tumor suppressor gene, has recently been reported to be ectopically expressed in primary adult T-cell leukemia–lymphoma (ATL) cells. We incorporated CADM1 into flow-cytometric analysis to reveal oncogenic mechanisms in human T-cell lymphotrophic virus type I (HTLV-I) infection by purifying cells from the intermediate stages of ATL development.

Experimental Design: We isolated CADM1- and CD7-expressing peripheral blood mononuclear cells of asymptomatic carriers and ATLs using multicolor flow cytometry. Fluorescence-activated cell sorted (FACS) subpopulations were subjected to clonal expansion and gene expression analysis.

Results: HTLV-I–infected cells were efficiently enriched in $CADM1^{+}$ subpopulations (D, $CADM1^{pos}CD7^{dim}$ and N, $CADM1^{pos}CD7^{neg}$). Clonally expanding cells were detected exclusively in these subpopulations in asymptomatic carriers with high proviral load, suggesting that the appearance of D and N could be a surrogate marker of progression from asymptomatic carrier to early ATL. Further disease progression was accompanied by an increase in N with a reciprocal decrease in D, indicating clonal evolution from D to N. The gene expression profiles of D and N in asymptomatic carriers showed similarities to those of indolent ATLs, suggesting that these subpopulations represent premalignant cells. This is further supported by the molecular hallmarks of ATL, that is, drastic downregulation of miR-31 and upregulation of abnormal *Helios* transcripts.

Conclusion: The CADM1 versus CD7 plot accurately reflects disease progression in HTLV-I infection, and $CADM1^{+}$ cells with downregulated CD7 in asymptomatic carriers have common properties with those in indolent ATLs. *Clin Cancer Res; 20(11); 2851–61. ©2014 AACR.*

Introduction

Human T-cell lymphotrophic virus type I (HTLV-I) is a human retrovirus that causes HTLV-I–associated diseases, such as adult T-cell leukemia–lymphoma (ATL), HTLV-I–associated myelopathy/tropical spastic paraparesis, and HTLV-I uveitis (1–3). In Japan, the estimated lifetime risk of developing ATL in HTLV-I carriers is 6% to 7% for males and 2% to 3% for females (4–6). It takes several decades for HTLV-I–infected cells to reach the final stage of multistep oncogenesis, which is clinically recognized as aggressive ATL (acute-type and lymphoma-type; ref. 7). Molecular interaction of viral genes [e.g., Tax and the HTLV-I basic leucine zipper (HBZ) gene] with the cellular machinery causes various genetic and epigenetic alterations (7–11). However, difficulties in purifying HTLV-I–infected cells *in vivo* seem to have hindered understanding of the genetic events that are directly involved in the multistep oncogenesis of ATL.

Upregulation or aberrant expression of cell surface markers, such as CCR4 and CD25, is useful for diagnosis of ATL and has been utilized for molecular-targeted therapy (12, 13). However, the expression levels of these markers vary among patients, which often make it difficult to identify ATL cells specifically based on the immunophenotype. Previously, we focused on downregulated markers in acute-type ATL cells, such as CD3 and CD7, and successfully purified ATL cells using the CD3 versus CD7 plot of $CD4^{+}$ cells (14). Analysis of other clinical subtypes

Authors' affiliations: [1]Division of Molecular Therapy; [2]Laboratory of Diagnostic Medicine, Division of Stem Cell Therapy; [3]Department of Hematology/Oncology, Research Hospital; [4]Clinical Laboratory, Research Hospital, Institute of Medical Science; and [5]Graduate School of Frontier Sciences, The University of Tokyo, Tokyo, Japan

Note: Supplementary data for this article are available at Clinical Cancer Research Online (http://clincancerres.aacrjournals.org/).

Corresponding Author: Kaoru Uchimaru, Institute of Medical Science, The University of Tokyo, 4-6-1 Shirokanedai, Minato-ku, Tokyo 108-8639, Japan. Phone: 81-3-5449-5542; Fax: 81-3-5449-5429; E-mail: uchimaru@ims.u-tokyo.ac.jp

doi: 10.1158/1078-0432.CCR-13-3169

Published OnlineFirst April 11, 2014; DOI: 10.1158/1078-0432.CCR-13-3169

Translational Relevance

In this study, we showed that the cell adhesion molecule 1 (CAMD1) versus CD7 plot reflects the progression of disease in patients infected with human T-cell lymphotrophic virus type I (HTLV-I), in that the proportion of $CADM1^{+}$ subpopulations (D, $CADM1^{pos}CD7^{dim}$ and N, $CADM1^{pos}CD7^{neg}$) increased with the progression from HTLV-I asymptomatic carrier (AC) to indolent adult T-cell leukemia–lymphoma (ATL) to aggressive ATL. We confirmed the purity of the clonal HTLV-I–infected cells in these subpopulations of various clinical subtypes, including asymptomatic carriers. The results from the flow-cytometric analysis will help physicians assess disease status. The analysis is also practical in screening for putative high-risk HTLV-I asymptomatic carriers, which show nearly identical flow-cytometric and gene expression profiles with those of smoldering-type ATL patients. Furthermore, cell sorting by flow cytometry enables purification of clonally expanding cells in various stages of oncogenesis in the course of progression to aggressive ATL. Detailed molecular analysis of these cells will provide valuable information about the molecular events involved in multistep oncogenesis of ATL.

(indolent ATLs and HTLV-I asymptomatic carriers; AC) revealed that HTLV-I–infected and clonally expanded cells were purified similarly and that the subpopulations with downregulated CD7 grew concomitantly with the progression of HTLV-I infection (15). Although this type of flow-cytometric analysis was shown to be a useful tool, a substantial subpopulation of T cells shows downregulated expression of CD7 under physiologic (16, 17) and certain pathologic conditions, including autoimmune disorders, viral infection, and hematopoietic stem cell transplantation (18–23).

Recently, Sasaki and colleagues reported ectopic overexpression of the cell adhesion molecule 1/tumor suppressor in lung cancer 1 (CADM1/TSLC1) gene in primary acute-type ATL cells based on expression profile analysis (24, 25). CADM1 (/TSLC1) is a cell-adhesion molecule that was originally identified as a tumor suppressor in lung cancers (25, 26). In addition, numbers of $CD4^{+}$ $CADM1^{+}$ cells have been found to be significantly correlated with the proviral load (PVL) in both ATLs and HTLV-I asymptomatic carriers (25, 27). Thus, CADM1 is a good candidate marker of HTLV-I–infected cells. In the present study, we incorporated CADM1 into our flow-cytometric analysis. In the CADM1 versus CD7 plot of $CD4^{+}$ cells, HTLV-I–infected and clonally expanded cells were efficiently enriched in the $CADM1^{+}$ subpopulations regardless of disease status. In these cells, stepwise CD7 downregulation (from dimly positive to negative) occurred with disease progression. The proportion of the three subpopulations observed in this plot [P, $CADM1^{negative(neg)}CD7^{positive(pos)}$; D, $CADM1^{pos}CD7^{dim}$; and N, $CADM1^{pos}$ $CD7^{neg}$] accurately reflected the disease status in HTLV-I infection. The analysis of comprehensive gene expression in each subpopulation revealed that the expression profile of $CADM1^{+}$ subpopulations in indolent ATLs showed similarities with that in asymptomatic carriers with high PVL; yet, it was distinct from that in aggressive ATLs. These D and N subpopulations were indicative of HTLV-I–infected cells in the intermediate stage of ATL development.

Materials and Methods

Cell lines and patient samples

TL-Om1, an HTLV-I–infected cell line (28), was provided by Dr. Sugamura (Tohoku University, Sendai, Japan). The MT-2 cell line was a gift from Dr. Miyoshi (Kochi University, Kochi, Japan) and ST-1 was from Dr. Nagai (Nagasaki University, Nagasaki, Japan). Peripheral blood samples were collected from in-patients and out-patients at our hospital, as described in our previous reports (14, 15). As shown in Supplementary Table S1, 26 cases were analyzed (10 cases of asymptomatic carrier; 5 cases of smoldering-type; 6 cases of chronic-type; and 5 cases of acute-type). All patients with ATL were categorized into clinical subtypes according to Shimoyama's criteria (12, 29). Patients with various complications, such as autoimmune disorders and systemic infections, were excluded. Lymphoma-type patients were also excluded because ATL cells are not considered to exist in the peripheral blood of this clinical subtype. Samples collected from six healthy volunteers (mean age 48.8 years; range 34–66 years) were used as normal controls. The present study was approved by the Institutional Review Board of our institute (the University of Tokyo, Tokyo, Japan). Written informed consent was obtained from all patients and healthy volunteers.

Flow cytometry and cell sorting

Peripheral blood mononuclear cells (PBMC) were isolated from whole blood by density gradient centrifugation, as described previously (14). An unlabeled CADM1 antibody (clone 3E1) and an isotype control chicken immunoglobulin Y (IgY) antibody were purchased from MBL. These were biotinylated (primary amine biotinylation) using biotin N-hydroxysuccinimide ester (Sigma-Aldrich). Pacific Orange-conjugated anti-CD14 antibody was purchased from Caltag-Invitrogen. All other antibodies were obtained from BioLegend. Cells were stained using a combination of biotin-CADM1, allophycocyanin (APC)-CD7, APC-Cy7-CD3, Pacific Blue-CD4, and Pacific Orange-CD14. After washing, phycoerythrin-conjugated streptavidin was applied. Propidium iodide (Sigma-Aldrich) was added to the samples to stain dead cells immediately before flow cytometry. A FACSAria instrument (BD Immunocytometry Systems) was used for all multicolor flow cytometry and fluorescence-activated cell sorting (FACS). Data were analyzed using FlowJo software (TreeStar). The gating

Published OnlineFirst April 11, 2014; DOI: 10.1158/1078-0432.CCR-13-3169

procedure for a representative case is shown in Supplementary Fig. S1.

Quantification of HTLV-I proviral load by real-time quantitative PCR

PVL in FACS-sorted PBMCs was quantified by real-time quantitative PCR (TaqMan method) using the ABI Prism 7000 sequence detection system (Applied Biosystems), as described previously (14, 30).

Evaluation of HTLV-I *HBZ* gene amplification by semiquantitative PCR

HTLV-I *HBZ* gene amplification was performed as described previously (25). Briefly, the 25-μL PCR mixture consisted of 20 pmol of each primer, 2.0 μL of mixed deoxynucleotide triphosphates (2.5 mmol/L each), 2.5 μL of 10× PCR buffer, 1.5 μL of $MgCl_2$ (25 mmol/L), 0.1 μL of AmpliTaq Gold DNA Polymerase (Applied Biosystems), and 20 ng of DNA extracted from cell lines and clinical samples. The PCR consisted of initial denaturation at 94°C for 9 minutes, 30 cycles of 94°C for 30 seconds, 57°C for 30 seconds, and 72°C for 45 seconds, followed by 72°C for 5 minutes. The β-actin gene (*ACTB*) was used as an internal reference control. The primer sequences used were as follows: HBZ forward, 5′-CGCTGCCGATCACGATG-3′; HBZ reverse, 5′-GGAGGAATTGGTGGACG-3′; ACTB forward, 5′-CGTGCTCAGGGCTTCTT-3′; and ACTB reverse, 5′-TGAAGGTCTCAAACATGATCTG-3′. Amplification with these pairs of oligonucleotides yielded 177-bp HBZ and 731-bp β-actin fragments.

FISH for quantification of HTLV-I–infected cells

FISH analysis was performed to detect HTLV-I proviral DNA in mononuclear cells that had been FACS-sorted on the basis of the CADM1 versus CD7 plot. These samples were sent to a commercial laboratory (Chromosome Science Labo Inc.), where FISH analysis was performed. Briefly, pUC/HTLV-I plasmid containing the whole-HTLV-I genome was labeled with digoxigenin by the nick translation method, and was then used as a FISH probe. Pretreatment, hybridization, and washing were performed according to standard laboratory protocols. To remove fluorochrome-labeled antibodies attached to the cell surface, pretreatment consisted of treatment with 0.005% pepsin and 0.1 N HCl. The FISH probe was detected with Cy3-labeled anti-digoxigenin antibody. Cells were counterstained with 4′, 6 diamidino-2-phenylindole. The results were visualized using a DMRA2 conventional fluorescence microscope (Leica) and photographed using a Leica CW4000 cytogenetics workstation. Hybridization signals were evaluated in approximately 100 nuclei.

Inverse long PCR to assess the clonality of HTLV-I–infected cells

For clonality analysis, inverse long PCR was performed as described previously (14). First, 1 μg genomic DNA extracted from the FACS-sorted cells was digested with *Pst*I or *Eco*RI at 37°C overnight. RNase A (Qiagen) was added to remove residual RNA completely. DNA fragments were purified using a QIAEX2 Gel Extraction Kit (Qiagen). The purified DNA was self-ligated with T4 DNA ligase (Takara Bio) at 16°C overnight. After ligation of the *Eco*RI-digested samples, the ligated DNA was further digested with *Mlu*I, which cuts the pX region of the HTLV-I genome and prevents amplification of the viral genome. Inverse long PCR was performed using Tks Gflex DNA Polymerase (Takara Bio). For the *Pst*I-treated group, the forward primer was 5′-CAGCCCATTCTATAGCACTCTCCAGGAGAG-3′ and the reverse primer was 5′-CAGTCTCCAAACACGTAGACTGGGTATCCG-3′. For the *Eco*RI-treated template, the forward primer was 5′-TGCCTGACCCTGCTTGCTCAACTCTACGTCTTTG-3′ and the reverse primer was 5′-AGTCTGGGCCCTGACCTTTTCAGACTTCTGTTTC-3′. Processed genomic DNA (50 ng) was used as a template. The reaction mixture was subjected to 35 cycles of denaturation (94°C, 30 seconds) and annealing plus extension (68°C, 8 minutes). Following PCR, the products were subjected to electrophoresis on 0.8% agarose gels. Fourteen patient samples were analyzed. For samples from which a sufficient amount of DNA was extracted, PCR was generally performed in duplicate.

Gene expression microarray analysis of each subpopulation in the CADM1 versus CD7 plot

Total RNA was extracted from each subpopulation in the CADM1 versus CD7 plot using TRIzol (Invitrogen) according to the manufacturer's protocol. Details of the clinical samples used for microarray analyses are shown in Supplementary Table S1. Treatment with DNase I (Takara Bio) was conducted to eliminate genomic DNA contamination. The quality of the extracted RNA was assessed using a BioAnalyzer 2000 system (Agilent Technologies). The RNA was then Cy3-labeled using a Low Input Quick Amp Labeling Kit (Agilent Technologies). Labeled cRNA samples were hybridized to 44K Whole Human Genome Oligonucleotide Microarrays (Agilent Technologies) at 65°C for 17 hours. After hybridization, the microarrays were washed and scanned with a Scanner C (Agilent Technologies). Signal intensities were evaluated by Feature Extraction 10.7 software and then analyzed using Gene Spring 12.0 software (Agilent Technologies). Unsupervised two-dimensional hierarchical clustering analysis (Pearson correlation) was performed on 10,278 genes selected by one-way ANOVA ($P < 0.05$). The dataset for these DNA microarrays has been deposited in Gene Expression Omnibus (accession number GSE55851).

Expression analysis of miR-31 and *Helios* transcript variants of each subpopulation in the CADM1 versus CD7 plot

The expression levels of the microRNA miR-31 were quantified using a TaqMan-based MicroRNA Assay (Applied Biosystems), as described previously (31), and normalized to RNU48 expression level. Helios mRNA transcript variants were examined using reverse transcription

Published OnlineFirst April 11, 2014; DOI: 10.1158/1078-0432.CCR-13-3169

PCR (RT-PCR) with Platinum Taq DNA Polymerase High Fidelity (Invitrogen), as described previously (32). To detect and distinguish alternative splicing variants, PCR analyses were performed with sense and antisense primer sets specific for the first and final exons of the Helios gene. The PCR products were then sequenced to determine the exact type of transcript variant. A mixture of Hel-1, Hel-2, Hel-5, and Hel-6 cDNA fragments was used as a "Helios standard" in the electrophoresis of RT-PCR samples.

Results

CADM1 expression based on the CD3 versus CD7 plot in CD4$^+$ cells in primary HTLV-I–infected blood samples

The clinical profiles of the 32 cases analyzed are shown in Supplementary Table S1. We first examined CADM1 expression in each subpopulation (H, I, and L) of the CD3 versus CD7 plot. Representative data (for a case of smoldering ATL) are shown in Fig. 1A. The results demonstrate that

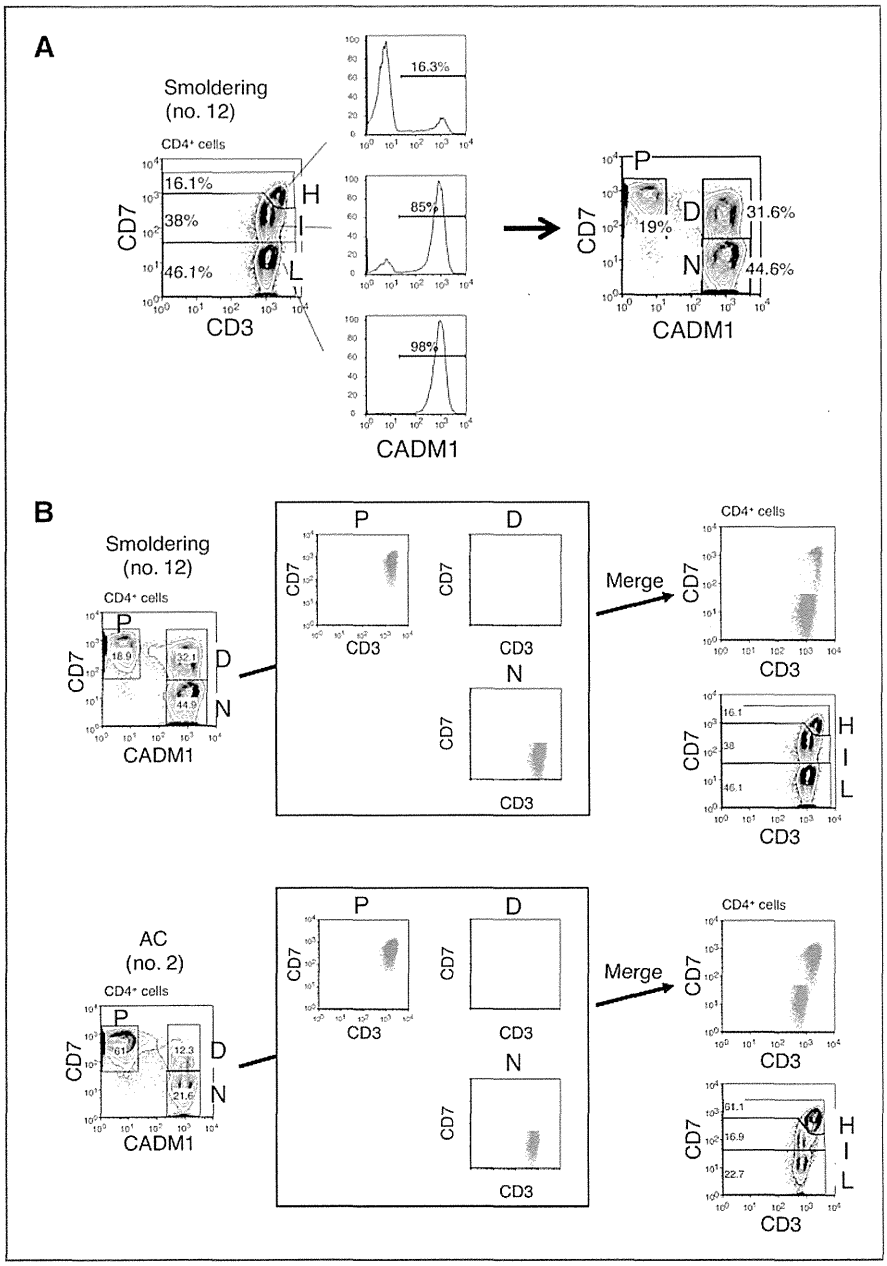

Figure 1. CADM1 versus CD7 plot for CD4$^+$ cells from HTLV-I–infected blood samples analyzed by flow cytometry. A, representative flow-cytometric analysis of a patient with smoldering-type ATL. Three subpopulations (H, I, and L) were observed in the CD3 versus CD7 plot for CD4$^+$ cells (left). Expression of CADM1 in each subpopulation is shown (middle). The right-hand panel shows how the CADM1 versus CD7 plot for CD4$^+$ cells was constructed. B, the P, D, and N subpopulations in the CADM1 versus CD7 plot correspond to the H, I, and L subpopulations in the CD3 versus CD7 plot. Blue, yellow, and red dots, respectively, indicate the P, D, and N subpopulations in the CADM1 versus CD7 plot, and are redrawn in the CD3 versus CD7 plot. Two representative cases are shown. In the upper case, the P and D subpopulations in the CADM1 versus CD7 plot are partly intermingled in the CD3 versus CD7 plot. Unlike the CD3 versus CD7 plot, the CADM1 versus CD7 plot clearly distinguishes three subpopulations.

Published OnlineFirst April 11, 2014; DOI: 10.1158/1078-0432.CCR-13-3169

CADM1 was expressed almost exclusively in the I and L subpopulations. Drawing a CADM1 versus CD7 plot for $CD4^+$ cells revealed three distinct subpopulations (P, $CADM1^{neg}CD7^{pos}$; D, $CADM1^{pos}CD7^{dim}$; and N, $CADM1^{pos}$ $CD7^{neg}$). As shown in Fig. 1B, the P, D, and N subpopulations corresponded to the H, I, and L subpopulations in the CD3 versus CD7 plot. In the previous CD3 versus CD7 plot, the lower case (AC no. 2) showed three distinct subpopulations. However, in the upper case (smoldering no. 12), the H and I subpopulations substantially intermingled with each other and were not clearly separated. In contrast, the CADM1 versus CD7 plot clearly revealed three distinct subpopulations in both cases.

HTLV-I–infected cells are highly enriched in $CADM1^+$ subpopulations

On the basis of previous reports (25, 27), we expected HTLV-I–infected cells to be enriched in the $CADM1^+$ subpopulations in our analysis. Figure 2A shows the PVL measurements of the three subpopulations in the CADM1 versus CD7 plot for three representative cases. HTLV-I–infected cells were highly enriched in the $CADM1^+$ subpopulations (D and N). The PVL data indicate that most of the cells in the D and N subpopulations were HTLV-I infected. Figure 2B shows the results of semiquantitative PCR of the *HBZ* gene in representative cases. In the D and N subpopulations, the *HBZ* gene was amplified to the same degree as in the HTLV-I–positive cell line. To confirm these results, FISH was performed in one asymptomatic carrier. As shown in Supplementary Fig. S2, HTLV-I–infected cells were highly enriched in the D and N subpopulations, which supports the results of the PVL analysis and semiquantitative PCR of the *HBZ* gene. In the FISH analysis, percentages of HTLV-I–infected cells in D and N did not reach 100%. This may have been due to a technical issue. Because the cells subjected to FISH analysis were sorted by FACS, several fluorochrome-conjugated antibodies may have remained on their surfaces, even after treatment with protease.

The CADM1 versus CD7 plot accurately reflects disease progression in HTLV-I infection

Compared with the CD3 versus CD7 plot, the CADM1 versus CD7 plot was revealed to be clear in its distinction of the three subpopulations and efficient in enrichment of HTLV-I–infected cells. On the basis of these findings, we analyzed clinical samples of asymptomatic carriers and three clinical subtypes of ATL: the smoldering, chronic, and acute subtypes. Data for representative cases, presented in Fig. 3A, suggest that the continual changes in the proportions of the three subpopulations are associated with disease progression. In the CADM1 versus CD7 plot, normal control samples showed a P-dominant pattern. With progression of the disease from the asymptomatic carrier state with a low PVL to that with a high PVL, and to indolent-type ATL, the D and N subpopulations increased gradually. As the disease further progressed to acute-type ATL, the N subpopulation showed remarkable expansion. Data for all analyzed samples are presented in Fig. 3B. The results suggest that the CADM1 versus CD7 plot of peripheral blood samples represents progression of the disease in HTLV-I carriers. Data for the normal control cases analyzed are shown in Supplementary Fig. S3. In all normal controls, the percentages of the D and N subpopulations were low. Supplementary Fig. S4 shows temporal data for a patient with chronic-type ATL who progressed from stable disease to a relatively progressive state and the concomitant change in the flow cytometry profile.

Clonality analysis of the three subpopulations in the CADM1 versus CD7 plot

To characterize the three subpopulations further, the clonal composition of each subpopulation was analyzed by inverse long PCR, which amplifies part of the provirus

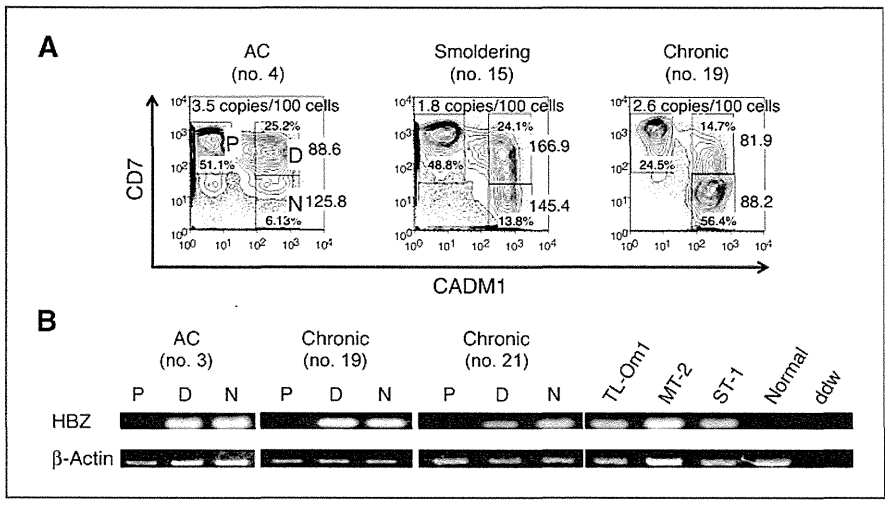

Figure 2. HTLV-I–infected cells are highly enriched in the $CADM1^+$ subpopulations. A, analysis of PVL in the three subpopulations. Three representative cases are shown. PVL data (copies/100 cells) are shown in red. Percentages of each subpopulation are shown in black. B, semiquantitative PCR of the *HBZ* gene in the three subpopulations in three representative cases. Normal, DNA from PBMCs from a normal control; ddw, deionized distilled water.

Published OnlineFirst April 11, 2014; DOI: 10.1158/1078-0432.CCR-13-3169

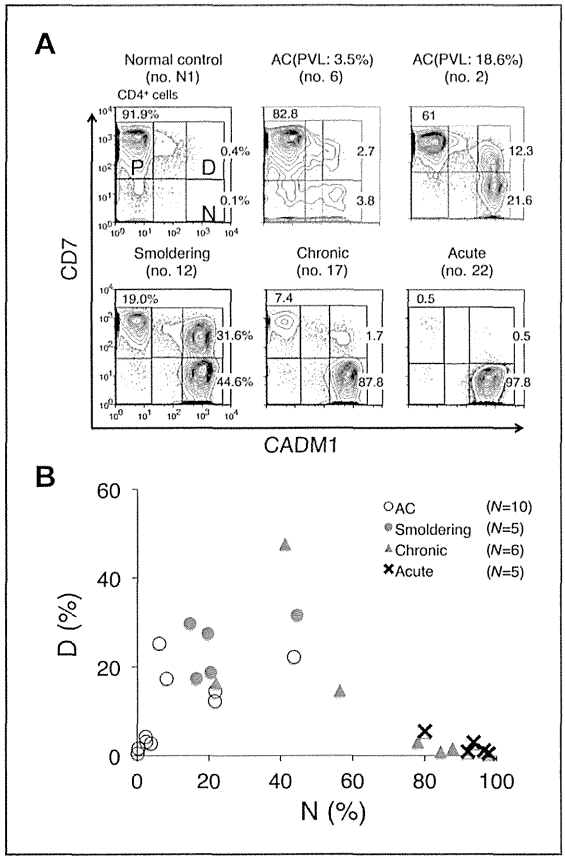

Figure 3. Proportion of each subpopulation in the CADM1 versus CD7 plots for asymptomatic HTLV-I carriers (asymptomatic carriers) and ATLs of various clinical subtypes. A, data of representative cases are shown. B, a two-dimensional plot of all analyzed samples showing the percentages of the D and N subpopulations.

long terminal repeat and the flanking genomic sequence of the integration sites. Cells in each subpopulation were sorted by FACS, and subjected to inverse long PCR analysis. Representative results for smoldering-, chronic-, and acute-type ATL samples are presented in Fig. 4A. Major clones, indicated by intense bands, were detected in the D and N subpopulations. The major clones in the D and N subpopulations in each case were considered to be the same based on the sizes of the amplified bands, suggesting that clonal evolution is accompanied by downregulation of CD7 expression. Fig. 4B shows representative results for three cases of asymptomatic carrier. In all cases, weak bands in the P subpopulation were visible, indicating that this population contains only minor clones. In these asymptomatic carriers, the proportion of abnormal lymphocytes and PVL increases from left to right. The consistent increase in the D and N subpopulations, together with growth of major clones as shown in the inverse PCR analysis, were considered to reflect these clinical data.

Gene expression profiling of the three subpopulations in the CADM1 versus CD7 plot

To determine the molecular basis for the biologic differences among the three subpopulations in the CADM1 versus CD7 plot, we next characterized the gene-expression profiles of the subpopulations of the following clinical subgroups: asymptomatic carriers ($n = 2$), smoldering-type ATLs ($n = 2$), chronic-type ATL ($n = 1$), acute-type ATLs ($n = 3$), and normal controls ($n = 3$). The two asymptomatic carriers (nos. 5 and 9) had high PVLs (11.6 and 26.2%, respectively) and relatively high proportions of D and N subpopulations (Supplementary Table S1). Unsupervised hierarchical clustering analysis of the results revealed three clusters (A, B1, and B2) or two major clusters A and B, where A is composed solely of the samples of the acute-type N subpopulation and B is subdivided into two clusters (B1 and B2; Fig. 5A). The B2 cluster is composed of the P subpopulation of all clinical subtypes and of normal controls, whereas the B1 cluster is composed of the D and N subpopulations of

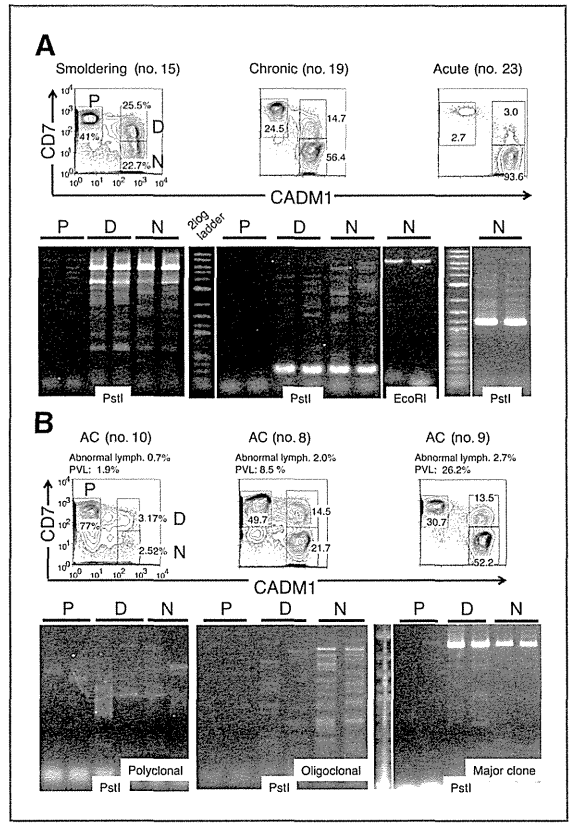

Figure 4. Clonality of subpopulations in the CADM1 versus CD7 plot analyzed by inverse long PCR. FACS-sorted cells (P, D, and N) were subjected to inverse long PCR. The black bar indicates duplicate data. Flow-cytometric profiles and clinical data are also presented. A, representative cases of smoldering-, chronic-, and acute-type ATL are shown. B, representative cases of asymptomatic carriers are shown.

Published OnlineFirst April 11, 2014; DOI: 10.1158/1078-0432.CCR-13-3169

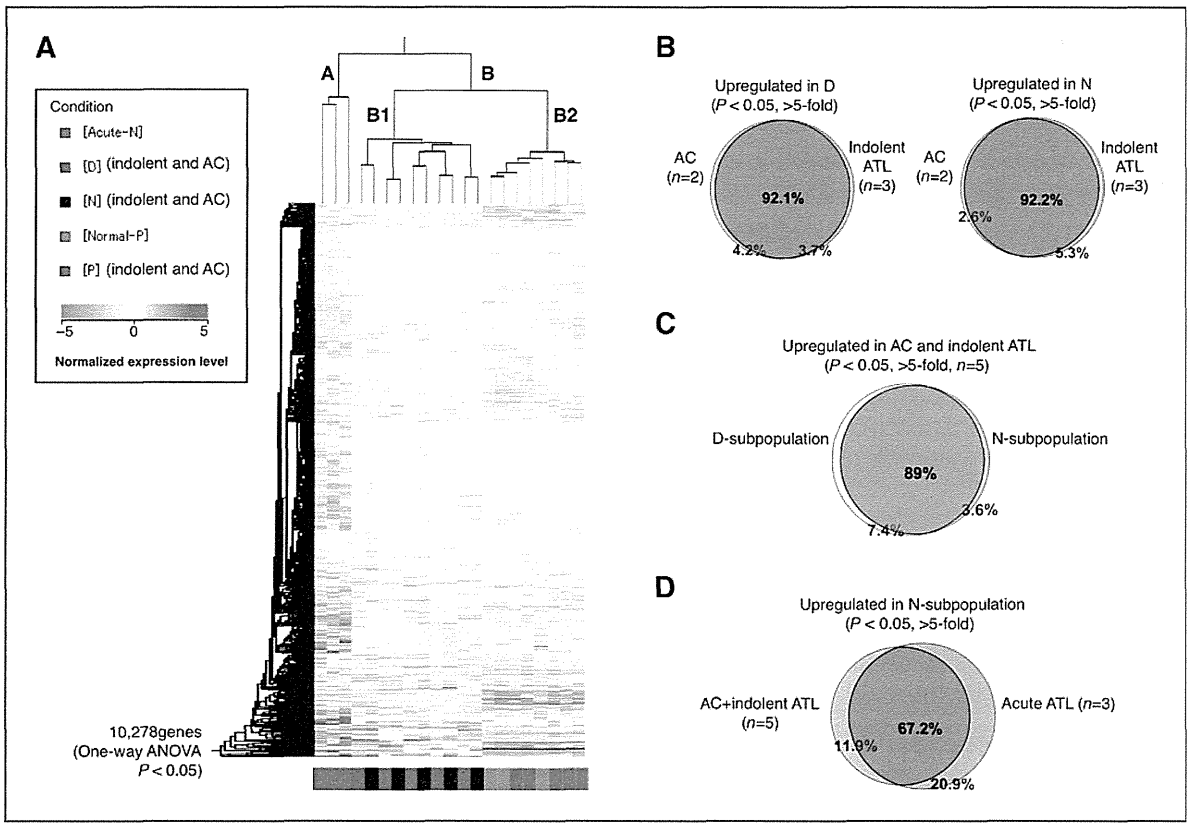

Figure 5. Comprehensive gene expression analysis of the three subpopulations in the CADM1 versus CD7 plot. A, we conducted an unsupervised hierarchical clustering analysis of 10,278 genes whose expression levels were significantly changed in the P subpopulation of normal controls ($n = 3$); P, D, and N subpopulations of asymptomatic carriers and indolent ATLs ($n = 5$); and N subpopulation of acute-ATLs ($n = 3$; one-way ANOVA, $P < 0.05$). The P and D subpopulations of acute ATLs and D and N subpopulations of normal controls could not be analyzed because of insufficient numbers of cells. Clustering resulted in three major clusters: (i) P subpopulations of normal controls (gray) and asymptomatic carriers/indolent ATLs (green); (ii) D and N subpopulations of asymptomatic carriers/indolent ATLs (blue and brown, respectively); and (iii) N subpopulations of acute ATLs (red). These results indicate that the P subpopulations of asymptomatic carriers/indolent ATLs have characteristics similar to those of normal uninfected cells, whereas the D and N subpopulations of asymptomatic carriers/indolent ATLs have genetic lesions in common. The N subpopulations of acute ATLs are grouped in an independent cluster, meaning that these malignant cell populations have a significantly different gene expression profile, even compared with the N subpopulations of indolent ATLs. B, similarity between asymptomatic carriers and indolent ATLs. The Venn diagrams show that 92.1% and 92.2% of genes upregulated in the D and N subpopulations, respectively, compared with "Normal-P" ($P < 0.05$), were common to asymptomatic carriers ($n = 2$) and indolent ATLs ($n = 3$). C, similarity between the D and N subpopulations. The Venn diagram shows that 89% of genes upregulated in the D and N subpopulation, compared with Normal-P ($P < 0.05$), overlapped. D, comparison of the N subgroups between acute-ATLs ($n = 3$) and asymptomatic carriers/indolent ATLs ($n = 5$). As shown in the Venn diagram, 67.2% of genes were upregulated ($P < 0.05$) in the N subpopulations of both acute ATLs and asymptomatic carrier/indolent ATLs. However, a significant number of genes (20.9%) were upregulated only in the N subpopulation of acute ATLs.

asymptomatic carriers and indolent ATLs (smoldering- and chronic-type).

Figure 5B shows a Venn diagram of the upregulated genes in the D subpopulation (left) or the N subpopulation (right) common to asymptomatic carriers ($n = 2$) and indolent ATLs ($n = 3$). These diagrams demonstrate that the changes in the gene expression profiles of the D and N subpopulations of asymptomatic carriers were similar to those of indolent ATLs. Furthermore, the gene expression profiles of the D and N subpopulations of asymptomatic carriers and indolent ATLs were similar (Fig. 5C). In contrast, the upregulated genes showed distinct differences between the N subpopulation of acute-type ATL and that of indolent ATLs and asymptomatic carriers, although approximately 70% were common to both (Fig. 5D).

Expression of a tumor suppressor microRNA and splicing abnormalities of Ikaros family genes in the three subpopulations

To determine whether the novel subpopulations identified had other properties in common with ATL cells, we examined miR-31 levels and *Helios* mRNA patterns in sorted subpopulations (31, 32). Expression of miR-31 decreased drastically in the D subpopulation derived from indolent ATLs and asymptomatic carriers, and was